STRUCTURAL AND FUNCTIONAL ANALYSES OF THE INTERACTION BETWEEN THE USP7-NTD AND THE E2-CONJUGATING ENZYMES, UBE2E2 AND UBE2E3

LEILA ASHUROV

A THESIS SUBMITTED TO THE FACULTY OF GRADUATE STUDIES IN PARTIAL FULFILLMENT OF THE REQUIREMENTS FOR THE DEGREE OF MASTER OF SCIENCE

GRADUATE PROGRAM IN BIOLOGY
YORK UNIVERSITY
TORONTO, ONTARIO

AUGUST 2014

ABSTRACT

Ubiquitin-specific protease 7 (USP7) is a deubiquitinating enzyme that regulates the turnover of proteins in a cell. To date several interacting partners that are involved in various cellular processes have been identified for USP7. Many of the interacting partners of USP7 contain a P/AxxS motif. We have identified two E2 ubiquitin-conjugating enzymes, UbE2E2 and UbE2E3, which contain the P/AxxS motif. Using a co-immunoprecipitation assay we have shown that these E2 proteins interact with USP7 through their P/AxxS motif. Co-crystal structures of the N-terminal domain of USP7 (USP7-NTD) and the E2 peptides reveal that the interactions are formed between USP7-NTD residues ^{164}DWGF^{167} and the E2 P/AxxS motifs. It has also been established that USP7 may be involved in regulating the cellular levels of UbE2E2. Overall, our findings suggest USP7, a de-ubiquitinating enzyme, is a regulator of ubiquitin-conjugating enzymes, which are involved in the ubiquitination cascade.

ACKNOWLEDGEMENTS

I would like to give my utmost gratitude to my Supervisor Dr. Vivian Saridakis. Thank you for taking me into your lab and providing me with this tremendous opportunity. Your constant support and guidance has allowed me to achieve my goals and complete this project. Thank you for sharing your knowledge with me and teaching me everything I know about USP7 and crystallography!

I would like to thank my Advisor Dr. Yi Sheng for dedicating your time and expertise to guide me through this project. I would also like to thank Dr. Michael Sheid and Dr. David A. Hood for taking the time out of your busy schedules to be a part of my thesis committee.

I am very grateful that I got the opportunity to be part of such an amazing lab where I have formed some memorable friendships. Thank you to Sara, Niharika, Ira, Jay, Feroz, Keith, Roland, Anna, Thaarshinee, Sanja, Mihai, Anuj, Tharanee, Rahima and Olga. All of you were of great help and support in the lab.

Finally, I would like to thank my mom, dad and brother for their love, support and constant encouragement.

TABLE OF CONTENTS

LIST OF TABLES

LIST OF FIGURES

LIST OF ABBREVIATIONS

AA Amino Acid

A	Ala	Alanine
C	Cys	Cysteine
D	Asp	Aspartic acid/Aspartate
E	Glu	Glutamic acid/Glutamate
F	Phe	Phenylalanine
G	Gly	Glycine
H	His	Histidine
I	Ile	Isoleucine
K	Lys	Lysine
L	Leu	Leucine
M	Met	Methionine
N	Asn	Asparagine
P	Pro	Proline
Q	Gln	Glutamine
R	Arg	Arginine
S	Ser	Serine
T	Thr	Threonine
V	Val	Valine
W	Trp	Tryptophan
Y	Tyr	Tyrosine

AMP	Adenosine monophosphate
ARA54	Androgen receptor-associated protein 54
ATP	Adenosine triphosphate
CHX	Cycloheximide
DUB	De-ubiquitinating enzyme
DMEM	Dulbecco's Modified Eagle's Medium
E1	Ubiquitin activating enzyme
E2	Ubiquitin conjugating enzyme
E3	Ubiquitin ligase
EBNA1	Epstein-Barr nuclear antigen 1
EBV	Epstein-Barr Virus
ECL	Enhanced chemiluminescence
FBS	Fetal bovine serum
GAPDH	Glyceraldehyde 3-phosphate dehydrogenase
GDM	Gestational Diabetes Mellitus
GFP	Green Fluorescent Protein
GMP	Guanosine monophosphate
GMPS	Guanosine monophosphate synthase
H2B	Histone protein 2B
HAUSP	Herpesvirus-associated ubiquitin-specific protease
HCT116	Human colorectal carcinoma cells

HDM2	Human double minute 2
HDMX	Human double minute X
HECT	Homologous to the E6-AP carboxyl terminus
HEK293T	Human embryonic kidney 293 cells with SV 40 Large T-antigen
hPAF	Human RNA polymerase II-associated factor
HSV	Herpes Simplex Virus
ICP0	Infected cell protein 0
IKKγ	Inhibitor of nuclear factor kappa-B kinase subunit gamma
JAMM	JAB1/MPN/Mov34 metalloenzyme
kDa	Kilodalton
MDM2	Murine double minute 2
MDMX	Murine double minute X
MJD	Machado-Josephin domain
NF-κB	Nuclear factor kappa-light-chain-enhancer of activated B cells
OTU	Ovarian tumour domain
PBS	Phosphate buffered saline
PBS-T	Phosphate buffered saline Tween
PCR	Polymerase chain reaction
Pfu	*Pyrococcus furiosus*
PVDF	Polyvinylidene difluoride
RING	Really interesting new gene
RNF8	Ring finger protein 8

RNF20/40	Ring finger protein 20/Ring finger protein 40 complex
RPE	Retinal epithelial cells
TLR	Toll-like receptor
TRAF	Tumour necrosis factor receptor-associated factor
TRAF6	Tumour necrosis factor receptor-associated factor 6
U2OS	Human osteosarcoma cells
Ub	Ubiquitin
UBC	Ubiquitin C
UbE2E1	Ubiquitin conjugating enzyme E2E 1
UbE2E2	Ubiquitin conjugating enzyme E2E 2
UbE2E3	Ubiquitin conjugating enzyme E2E 3
UbE2K	Ubiquitin conjugating enzyme E2 K
UBL	Ubiquitin-like
UCH	Ubiquitin C-terminal hydrolases
USP	Ubiquitin specific protease
USP7	Ubiquitin specific protease 7
USP7-CS	USP7 catalytic mutant (C223S)
USP7-CTD	USP7 C-terminal domain
USP7-DW	USP7 binding mutant (D164A/W165A)
USP7-NTD	USP7 N-terminal domain
USP7-WT	USP7 wild-type
USP8	Ubiquitin specific protease 8

CHAPTER 1: INTRODUCTION

1.1 Ubiquitin

Ubiquitin is an 8.5 kDa protein that is highly conserved amongst eukaryotes (Goldstein et al., 1975). The critical elements of its sequence include a di-glycine motif at the C-terminal end and seven lysine residues occurring at positions 6, 11, 27, 29, 33, 48 and 63 (Figure 1.1). Ubiquitin is expressed as either a polyubiquitin chain or as a fusion protein with an essential ribosomal polypeptide (Kimura and Tanaka, 2009). In mammals ubiquitin is encoded by 4 genes; Ubb, Ubc, Uba52 and Uba80, two of which encode the polyubiquitin and two of which encode the ribosomal fusion ubiquitin. Although ubiquitin is abundant in all eukaryotic cells, it is highly regulated by ubiquitin encoding genes, by a change in proteasome composition and by de-ubiquitinating enzymes (Kimura and Tanaka, 2009).

In a process called ubiquitination, ubiquitin is conjugated to a lysine residue on a substrate protein at a single site or as a polymer formed by the polymerization of ubiquitin monomers (Pickart, 2001). Ubiquitination can induce cellular processes such as protein degradation, endocytosis, DNA repair, chromatin remodeling and initiation of inflammatory response (Pickart, 2001). The type of cellular process induced depends on the amount of ubiquitin molecules attached to the protein and the topology of the ubiquitin chain, which depends on the lysine residue used for attachment. For example, a ubiquitin chain linked by K48 will target the modified protein for degradation by the 26S proteasome (Peng et al., 2003).

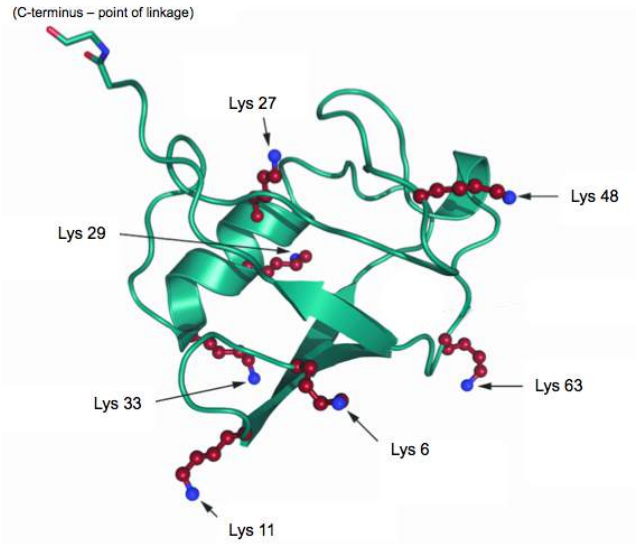

Figure 1.1: Ubiquitin is a 76 amino acid polypeptide. Ubiquitin is attached to a protein substrate in a process called ubiquitination. The crucial elements of its structure are a di-glycine motif at the C-terminal end (point of attachment) and seven lysine residues located at positions 6, 11, 27, 29, 33, 48 and 63. The figure was retrieved and modified from Komander (2009).

1.2 Ubiquitination

Ubiquitination is a post-translational modification in which a ubiquitin molecule is added to a substrate protein. Ubiquitination is a three-step process that involves the cooperative action of three enzymes; ubiquitin-activating enzyme (E1), ubiquitin-conjugating enzyme (E2) and ubiquitin ligase (E3) (Figure 1.2). First, E1 catalyzes the acyl-adenylation of the C-terminus of ubiquitin, forming an ubiquitin-adenylate intermediate that is ready for nucleophillic attack. The ubiquitin-adenylate intermediate is then transferred to the cysteine residue in the E1 active site creating a thioester bond between the carboxyl group of G76 in ubiquitin and the sulfhydryl group of the catalytic cysteine of E1. The activated thiol- linked ubiquitin is transferred to the catalytic

cysteine of E2 (Pickart, 2001). E2-ubiquitin interacts with E3, which recognizes a specific protein substrate and mediates the transfer of the activated ubiquitin molecule on E2 to the protein substrate (Passmore and Barford, 2004). The way in which the ubiquitin molecule is transferred from the E2 to the substrate protein depends on the presence of either a HECT domain or a RING finger in the E3. When a HECT domain is present in the E3, the ubiquitin molecule is transferred from the E2 to the active site cysteine of the E3. The ubiquitin molecule is then transferred from the E3 to the substrate protein (Passmore and Barford, 2004). On the other hand, RING finger E3s act as a scaffold, facilitating the transfer of ubiquitin from the E2 to the substrate protein (Passmore and Barford, 2004). The protein substrate and the ubiquitin molecule are attached by an isopeptide bond that is formed between the carboxyl group of G76 on ubiquitin and the ε-amino of a lysine in the substrate protein (Pickart, 2001). The process of ubiquitination can terminate forming a monoubiquitinated protein or it can continue forming an ubiquitin polymer, in which the G76 of the incoming ubiquitin is attached to one of seven lysine residues on the attached ubiquitin (Figure 1.2).

In humans there are six different E1s, approximately 35 different E2s and over one thousand E3s (van Wiljk and Timmers, 2010). Compared to E3s, E2s are comprised of a much smaller number of enzymes and there remains a gap in the knowledge about their function and the molecular mechanisms involved in their regulation.

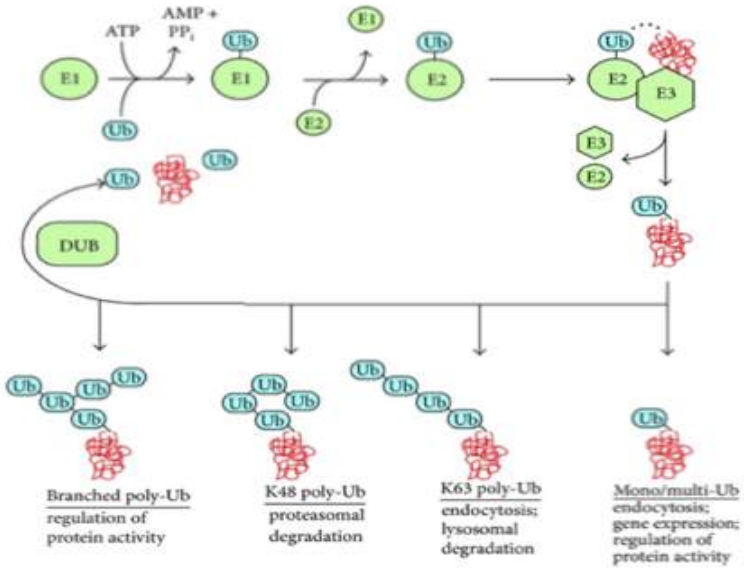

Figure 1.2: Ubiquitination involves the cooperation of three enzymes. Ubiquitination is a post-translational modification that is facilitated by the cooperative action of three enzymes; ubiquitin-activating enzyme (E1), ubiquitin-conjugating enzyme (E2) and ubiquitin ligase (E3). The fate of the substrate protein depends on the amount and topology of ubiquitin molecules attached. Ubiquitination is reversible. The reversal of ubiquitination is catalyzed by deubiquitinating enzymes (DUBs). This image was retrieved from Hamilton and Zito, 2013.

1.3 Ubiquitin-Conjugating Enzymes (E2s)

1.3.1 Function of E2s

E2s are the second enzyme in the ubiquitination cascade. E2s bind an E1-activated ubiquitin via their catalytic cysteine residue. The E2-ubiquitin conjugate then selectively interacts with a specific E3 ligase, which recruits a protein substrate to be ubiquitinated. E2 enzymes play a role in determining which of the seven-lysine residues in ubiquitin are used in polyubiquitination, thereby influencing the fate of the substrate protein (David et al., 2010). Different E2 enzymes have a different preference for which

lysine residue is used for polyubiquitination; the most commonly used lysine residues are lysine 11, 48 and 63 (David et al., 2010). It has been shown that polyubiquitin chains are formed at the active site cysteine in the E2 enzyme and are transferred from the E2 to the substrate protein (Li et al., 2007; David et al., 2010). If a substrate protein is tethered to an E2 enzyme, the E2 enzyme could ubiquitinate the substrate in absence of an E3 ligase. However, the type of ubiquitin conjugate and the identity of the target lysine residue on the substrate protein are not specific (David et al., 2011).

1.3.2 Localization of E2s

Most E2s are expressed in a variety of cell types and tissues; however, some are predominantly expressed in specific tissues. For example, UbE2K is highly expressed in certain regions of the brain (van Wiljk and Timmers, 2010). Inside the cell, E2s are present in both the nucleus and the cytoplasm. When tagged with a ubiquitin, certain E2s can be transported from the cytoplasm to the nucleus by the transport receptor importin-11 (Plafker et al., 2004).

1.3.3 Structure of E2s

E2s have an evolutionarily conserved, ~150-200 amino acid ubiquitin-conjugating catalytic fold (UBC) (Burroughs et al., 2008). The UBC fold consists of a four-stranded antiparallel β-sheet that is flanked by one α-helix at the N-terminal end (helix 1) and two α-helices at the C-terminal end (helices 2a and 2b) (Burroughs et al., 2008; Wenzel et al.,

2011; Figure 1.3A). Loop 1 and loop 2, which connect β-strand 1 and 2 and β-strand 3 and 4, respectively, have a lot of sequence variability amongst E2s and are thought to be involved in selectively binding E3s (van Wiljk and Timmers, 2010). The active site cysteine is positioned in the highly conserved loop region connecting helix 2 with β-strand 4 (Burroughs et al., 2008; van Wiljk and Timmers, 2010). Within ten residues upstream of the active site cysteine lays a highly conserved HxN sequence. It is thought that the histidine maintains the structure of the active site and the asparagine is involved in catalysis of the isopeptide bond formed between the ubiquitin in the active site and the substrate protein (Wenzel et al., 2011).

E2s are classified into four families based on their structural organization. Class I E2s consist only of a UBC fold; class II E2s have a UBC fold and a C-terminal extension; class III E2s have a UBC fold and a N-terminal extension; and class IV E2s have a UBC fold and both a C- and N-terminal extension. Unlike the UBC fold, which is 95% conserved amongst all E2 families, the extensions are not conserved. These extensions account for functional differences amongst E2s, as well as differences in subcellular localization (van Wiljk and Timmers, 2010).

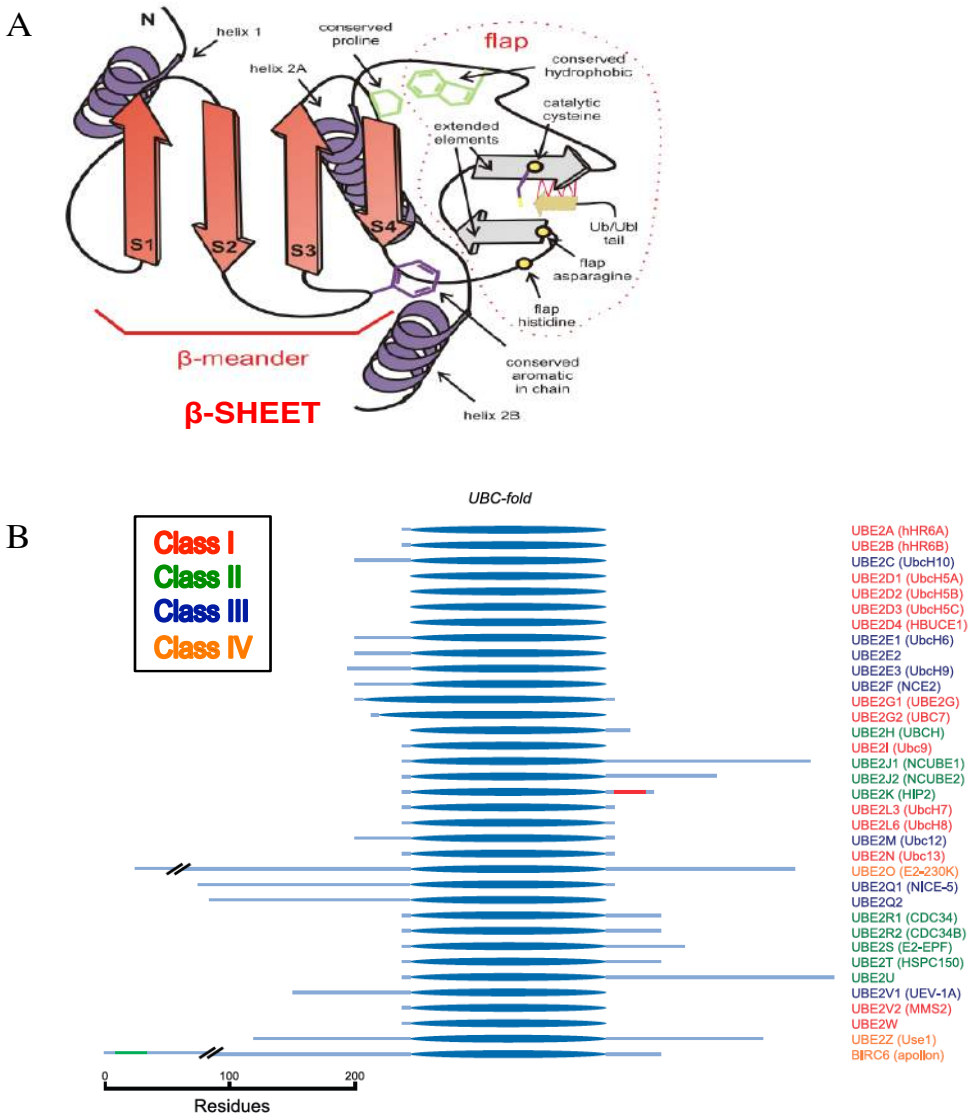

Figure 1.3: E2s have a conserved UBC fold and are divided into four classes based on their structure. (A) The UBC fold has 3 α-helices; one at the N-terminus (helix 1) and two at the C-terminus (helix 2a and 2b). The α-helices surround an antiparallel, 4-stranded β-sheet and a C-terminal flap that contains two extended elements. The catalytic cysteine is located in an exposed region of the flap (yellow). The conserved histidine and asparagine elements are located in the N-terminal region of the flap (yellow). All other conserved residues are depicted in stick form. This figure was retrieved and altered from Burroughs et al. (2009). (B) E2s are divided into 4 classes based on their structure. Class I E2s have only a UBC fold; class II E2s have a C-terminal extension; Class III E2s have an N-terminal extension; and class IV E2s have both a C and N-terminal extension. This figure was retrieved and altered from van Wiljk and Timmers, (2010).

1.4 Class III Ubiquitin-Conjugating Enzymes

The human genome encodes nine class III ubiquitin-conjugating enzymes (class III E2s) (van Wiljk and Timmers, 2010). Class III E2s are characterized by the presence of an N-terminal extension. The UBC fold of the class III E2s is 94% conserved amongst eukaryotes and is composed of approximately 149 amino acid residues (Matuschewski et al., 1996). In contrast to the UBC fold, the N-terminal extensions of the class III E2s bear little sequence similarity and differ in size (Matuschewski et al., 1996). The minimal sequence similarity between the N-terminal extensions comes from clusters of serine and threonine residues (Matuschewski et al., 1996).

The class III E2s UbE2E1, UbE2E2 and UbE2E3 have 97% sequence similarity over the 143 amino acid residues in their UBC domain. The high sequence similarity between their UBC domains gives these three enzymes overlapping properties. First, a ubiquitin-charged form of these enzymes can be transported to the nucleus via the importin-11 transport receptor (Plafker et al., 2004). Second, these enzymes share common E3-ligase binding partners such as ARA54, RNF8 and cullin-3 E3 ligases (Ito et al. 2001; Plafker et al. 2009). In contrast to their UBC domain, their N-terminal extensions vary in length and have little sequence similarity (Figure 1.4). Schumacher et al. (2013) have recently shown that the N-terminal extension of the UbE2E enzymes limits ubiquitin transfer. In an experiment with the UBC fold alone, the UbE2E enzymes were able to polyubiquitinate a substrate. However, the full-length protein was only able to monoubiquitinate the same substrate (Schumacher et al., 2013). Although the N-terminal extension limits the ubiquitin transfer potential of all three

UbE2E enzymes, the lack of sequence similarity in these extensions is the factor determining the substrate specificity and unique function of these enzymes.

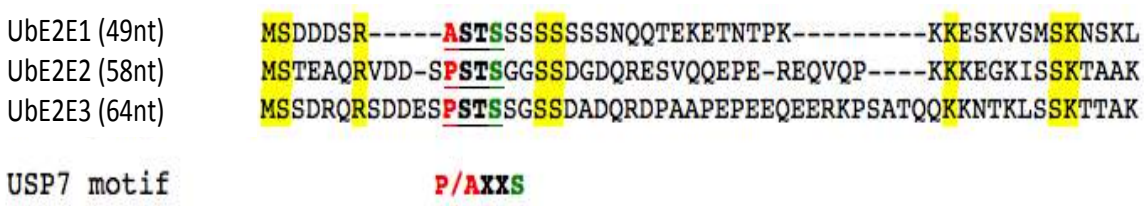

Figure 1.4: The N-terminal extensions of the UbE2E proteins bear little sequence similarity. A sequence alignment of the N-terminal extensions of the UbE2E proteins shows little sequence similarity. Residues highlighted in yellow are conserved amongst the three proteins. The USP7 substrate recognition motif, PSTS is also conserved amongst the three proteins.

1.4.1 UBE2E1

UbE2E1 is a 21.4 kDa protein with a N-terminal extension that is 49 amino acid residues in length. UbE2E1 has been implicated in histone ubiquitination. It has been shown that UbE2E1 interacts with RNF20/40, an E3 ligase, and the hPAF complex to monoubiquitinate lysine 120 in Histone 2B (H2B). The mono-ubiquitination promotes expression of HOX genes (Zhu et al., 2005).

1.4.2 UbE2E2

UbE2E2 is a 22.3 kDa protein with a N-terminal extension that is 58 amino acid residues in length. Aside from acting as a ubiquitin-conjugating enzyme, not much is known about the function of UbE2E2. However, a recent genetic association study has implicated UbE2E2 in gestational diabetes mellitus (GDM). The study showed that one

of two single-nucleotide polymorphisms for UbE2E2 showed a significant association with GDM in a recessive model (Kim et al., 2013).

1.4.3 UbE2E3

UbE2E3 is a 22.9 kDa protein with a N-terminal extension that is 64 amino acid residues in length. In the past decade, much has been uncovered about the function of UbE2E3. Plafker et al. (2008) implicated UbE2E3 as an essential enzyme involved in the proliferation of retinal pigment epithelial (RPE) cells. Furthermore, UbE2E3 was implicated in restoring redox homeostasis after oxidative stress (Plafker et al., 2010). Although there is some insight regarding the function of the class III E2 enzymes, not much is known about their regulation.

1.5 De-Ubiquitinating Enzymes (DUBs)

Ubiquitination is a reversible process. Reversibility of ubiquitination is facilitated by a group of enzymes known as de-ubiquitinating enzymes (DUBs). DUBs remove ubiquitin or ubiquitin-like proteins from pro-proteins and conjugates by hydrolyzing the, thioester and amide bonds at G76 of ubiquitin.

1.5.1 The Role of DUBs in the Cell

DUBs play several roles in the cell. First, they process primary ubiquitin gene products (Reyes-Turcu, 2009). Ubiquitin is expressed either in the form of a polyubiquitin chain or fused to one of the two ribosomal proteins. In order for ubiquitin to become a mature protein, it must be processed into a monomer. DUBs process the ubiquitin pro-protein to produce an active monomer (Reyes-Turcu, 2009). Second, DUBs reverse the ubiquitin or ubiquitin-like modification of target proteins by removing the ubiquitin or ubiquitin like moiety, therefore, salvaging the target protein from its eventual fate (Reyes-Turcu, 2009). Third, DUBs are responsible for recycling of ubiquitin (Kim et al., 2003). Following degradation of the target protein by the 26S proteasome, DUBs disassemble polyubiquitin chains and remove protein remnants to produce ubiquitin monomers that are reused in the ubiquitination cascade (Kim et al., 2003). Finally, DUBs can edit the topology of the ubiquitin chain, thus preventing inappropriate ubiquitin signaling (Kim et al., 2003).

1.5.2 Classification of DUBs

The Human Genome Project has identified almost 100 putative DUBs. These DUBs are classified into two families based on their mechanism of catalysis: cysteine proteases and metalloproteases. The cysteine protease family is further divided into four super families: ubiquitin C-terminal hydrolases (UCH), ubiquitin specific proteases (USP/UBP), the ovarian tumor domain (OTU) and Machado-Josephian domain (MJD)

(Reyes-Turcu, 2009). The metalloprotease family is comprised of one zinc-dependent superfamily JAB1/MPN/Mov34 (JAMM) (Reyes-Turcu, 2009).

The largest superfamily of DUBs is the USP/UBP superfamily. DUBs in this superfamily have a highly conserved 350 amino acid core domain, which is comprised of three subdomains called finger, palm and thumb (Kim et al., 2003). The core domain has a variety of N-terminal and C-terminal extensions and insertions and contains a catalytic cysteine (Kim et al., 2003). The region surrounding the catalytic cysteine is homologous amongst the members of this superfamily and contains a Cys and His box (Kim et al., 2003). One of the proteins studied in this project is a DUB belonging to the USP/UBP superfamily called Ubiquitin Specific Protease 7 (USP7).

1.6 Ubiquitin Specific Protease 7 (USP7/HAUSP)

Ubiquitin-Specific Protease 7 (USP7) was first identified as a 135 kDa protein that binds to the Herpes Simplex Virus protein, ICP0 (Meredith et al., 1994). For this reason it was named Herpesvirus Associated Ubiquitin Specific Protease (HAUSP). USP7 is conserved throughout eukaryotic evolution and is expressed in a variety of cell types (Everett et al., 1997).

1.6.1 Domains

USP7 is an 1102 amino acid protein and is comprised of three domains; N-terminal domain (NTD), catalytic domain and C-terminal domain (CTD) (Figure 1.5). The catalytic domain spans residues 208-560 and is composed of three sub-domains:

finger, thumb and palm (Hu et al., 2002). Like other USP proteins, the catalytic domain of USP7 contains a conserved Cys and His box (Hu et al., 2002). The Cys box contains the catalytic cysteine, Cys223, which gets deprotonated and unleashes nucleophillic attack on the carbonyl carbon atom of Gly76 in ubiquitin (Hu et al., 2002). The deprotonation of the Cys223 is facilitated by an adjacent His464 residue, which is stabilized by a nearby Asn or Asp residue. Together these three residues comprise the catalytic triad and sit in a site called the catalytic cleft (Hu et al., 2002). Upon binding of ubiquitin the structure of the catalytic cleft changes to bring the Cys and His residues in closer proximity (Hu et al., 2002).

A TRAF homology domain at the N-terminus and five ubiquitin-like (UBL) domains at the C-terminus surround the catalytic domain (Figure 1.5). The TRAF-like NTD spans residues 54-205 and forms an eight-stranded, anti parallel β-sandwich (Saridakis et al., 2005). The NTD has been implicated in substrate recognition and interaction (Saridakis et al., 2005, Sheng et al 2006). The five UBLs span residues 560-1102 and together comprise the CTD (Faesen et al., 2011). Functional analysis of USP7 showed that the CTD is required for full activity of the enzyme. Specifically, UBL4 and UBL5 activate the catalytic domain and promote ubiquitin binding (Faesen et al., 2012).

A

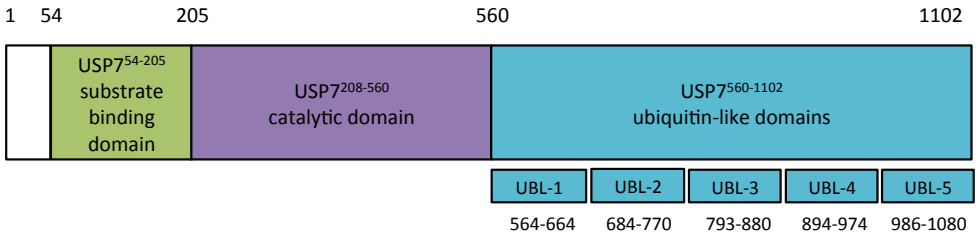

B

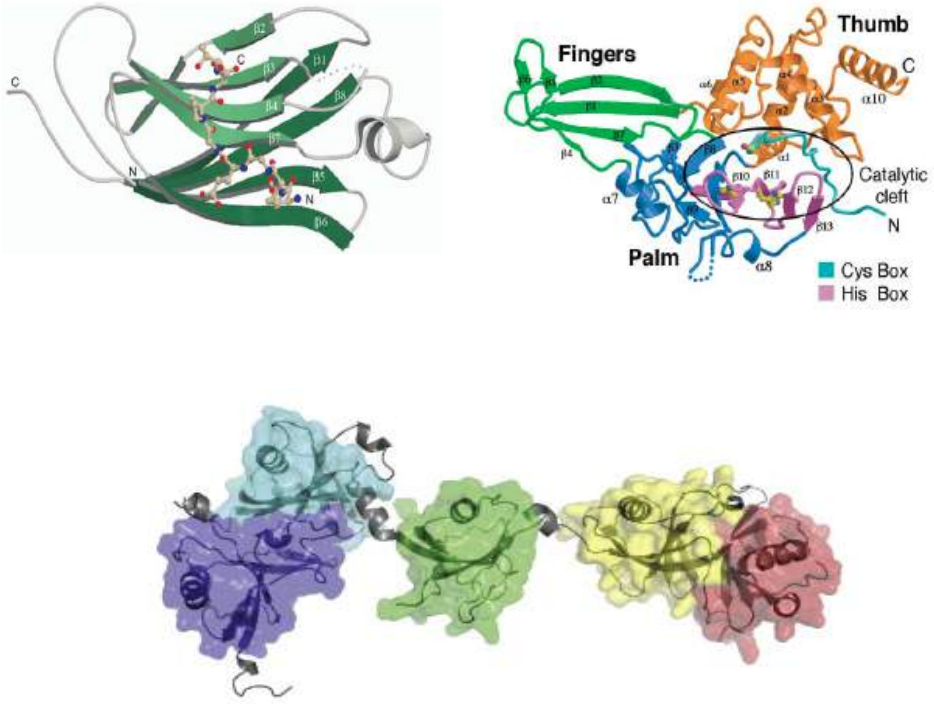

Figure 1.5: USP7 is an 1102 amino acid protein with 3 domains. (A) USP7 is a 135 kDa protein that is comprised of 1102 amino acids and 3 domains. The N-terminal domain spans from amino acids 54-205 and is involved in substrate binding. The catalytic domain contains an active site cysteine and spans amino acids 208-560. The C-terminal (CTD) domain is the largest and spans amino acids 560-1102. The CTD consists of 5 ubiquitin-like domains (UBLs). Each UBL is structurally homologous to ubiquitin but lacks glycine 76. (B) The crystal structures of the N-terminal domain (top left), catalytic domain (top right) and C-terminal domain (bottom) were determined by (Saridakis et al., 2005), (Hu et al., 2002) and (Faesen et al., 2011), respectively.

1.6.2 Cellular Function of USP7

USP7 has been implicated in several cellular processes such as tumour suppression, viral infection, immune response, DNA damage response and epigenetics. Perhaps it is best known for its dynamic role in the p53-Mdm2 tumor suppression pathway. Under regular cellular conditions, p53 levels are kept low by the E3 ubiquitin ligase Mdm2, which mediates the ubiquitylation and subsequent degradation of p53 (Moll and Petrenko, 2003). Upon oncogenic stress, p53 levels are strongly stabilized via deubiquitination by USP7, allowing for p53-dependent cell growth repression and apoptosis (Li et al., 2002). This demonstrates a tumour suppressor function for USP7. Interestingly, USP7 has also been implicated in stabilizing the p53 antagonist Mdm2 suggesting that it is involved in a feedback loop that regulates p53 function (Li et al., 2004).

In addition to its role as a tumor suppressor, USP7 has been shown to interact with viral proteins. One such protein is Epstein Barr Nuclear Antigen 1 (EBNA1), which interacts with the USP7-NTD (Holowaty et al., 2003). EBNA1 competes with tumour suppressor p53 for USP7 binding (Saridakis et al., 2005). By binding to the USP7-NTD, EBNA1 prevents p53-dependent cell cycle arrest and apoptosis, allowing for cell immortalization by the Epstein Barr Virus (Saridakis et al., 2005).

While EBNA1 binds to the NTD of USP7, another viral protein called ICP0 interacts with the CTD of USP7. ICP0 is a Herpes Simplex Virus (HSV) immediate early protein. Unlike EBNA1, which binds to USP7 to prevent it from performing its function

as a deubiquitinase, ICP0 binds USP7 to facilitate its export to the cytoplasm where it modulates Toll-like Receptor (TLR) mediated innate immune response (Daubeuf et al., 2009). One way in which TLRs mediate innate immune response is through a signaling pathway that activates the transcription factor NF-κB, which in turn transcribes inflammatory cytokines (Kawai and Akira, 2007). TRAF6 and IKKγ are two components of the TLR signaling pathway that lead to activation of NF-κB. TRAF6 is an E3 ligase that ubiquitinates itself and IKKγ. Ubiquitinated TRAF6 and IKKγ eventually lead to the activation of NF-κB (Kawai and Akira, 2007). ICP0 recruits USP7 to the cytoplasm, where it binds and deubiquitinates TRAF6 and IKKγ, preventing NF-κB mediated inflammatory response (Daubeuf et al., 2009). Exploitation of USP7 by the viral protein ICP0 allows HSV to bypass innate immune response (Daubeuf et al., 2009).

Moreover, USP7 has been implicated in epigenetic silencing. USP7 interacts with a metabolic enzyme called GMP synthase (GMPS). The interaction between USP7 and GMPS leads to deubiquitination of monoubiquitinated histone H2B (uH2B), which in turn leads to epigenetic silencing of homeotic genes in *Drosophila* (van der Knapp et al., 2005).

1.6.3 Substrates and Interacting Motif of the USP7-NTD

USP7 interacts with the Epstein-Barr nuclear antigen 1 (EBNA1) through an ^{444}EGPS^{447} motif in the EBNA1 protein (Saridaks et al., 2005). The most essential residues involved in the interaction were Glu444 and Ser447 in EBNA1 and Asp164 and Trp165 in USP7. Further studies with the USP7-NTD revealed that a ^{359}PGGS^{362} motif in p53 was essential for binding to the USP7-NTD (Sheng et al., 2006). Pro359 and S362 were most critical to this interaction as mutation of either residue reduced the binding up to two-fold and a double mutant reduced binding three-fold (Sheng et al., 2006). Examination of the p53 protein sequence revealed another motif (^{364}AHSS^{367}) that is critical for the interaction with USP7-NTD. In this motif Ala364 mediates the same interactions with USP7-NTD as does Pro359 and Ser367 mediates the same contacts as Ser362 (Sheng et al., 2006). Similar binding motifs were found in Mdm2 (^{156}PSTS^{159}, ^{147}PSSS^{150}), where the proline and serine were critical for binding (Sheng et al., 2006). This allowed for the identification of a consensus-binding motif, P/AxxS, for USP7-NTD substrates. Following the identification of the P/AxxS consensus motif, several other interacting partners of the USP7-NTD were discovered such as HdmX (Sarkari et al., 2010), UbE2E1 (Sarkari et al., 2013), MCM-BP (Jagannathan et al., 2014) and CHFR (Luthra et al., unpublished), all of which contain this consensus sequence. Figure 1.6 shows the USP7-NTD substrates and their P/AxxS consensus sequence.

A ^{164}DWGF^{167} motif in the USP7-NTD was shown to be essential for binding to substrates containing the P/AxxS motif (Sheng et al 2006). USP7-NTD Trp165 has a major role and USP7-NTD Asp164 has a minor role in binding to substrates (Sheng

et al., 2006). This was confirmed when substrate binding was abolished upon mutation of Trp165 and reduced two-fold upon mutation of Asp164 (Sheng et al., 2006).

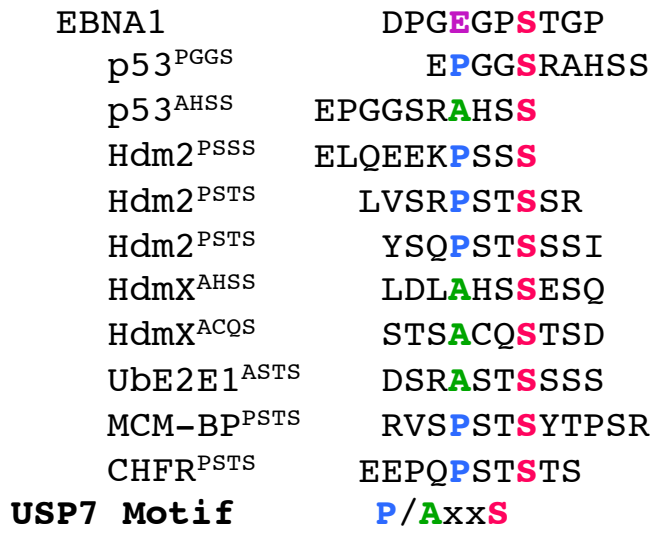

Figure 1.6: USP7 substrates contain a P/AxxS motif. Several USP7 substrates that bind to the USP7-NTD contain a P/AxxS binding motif that is required for binding to the USP7 protein.

1.6.4 USP7 Interacts with the Class III Ubiquitin-conjugating Enzyme UbE2E1

It has recently been demonstrated that the class III ubiquitin-conjugating enzyme UbE2E1 binds to the USP7-NTD. Analysis of the UbE2E1 protein sequence revealed that its N-terminal extension contains the USP7 binding motif P/AxxS (Sarkari et al., 2013). Using a GST-pull down assay, Sarkari et al. (2013) showed that UbE2E1 interacts with USP7 via the ^{8}ASTS^{11} motif in its N-terminal extension and the ^{164}DWGF^{167} motif in the USP7-NTD. The interaction between UbE2E1 and USP7 was further validated *in vivo*

using a coimmunoprecipitation assay (Sarkari et al., 2013).

The detailed molecular mechanism of interaction between USP7 and UbE2E1 was determined through x-ray crystallography. Sarkari et al. (2013) determined the structure of the USP7-NTD in complex with a UbE2E1 peptide containing the P/AxxS binding motif. The structure confirmed that the interaction occurs between ^{8}ASTS^{11} in UbE2E1 and ^{164}DWGF^{167} in the USP7-NTD. Ser^{11} of UbE2E1 made the most contacts with the USP7-NTD, forming two hydrogen bonds with Asp^{164} of USP7 (Sarkari et al., 2013).

Sarkari et al. (2013) also demonstrated the effect of the USP7:UbE2E1 interaction. An *in vitro* ubiquitination assay revealed that in the presence of USP7, UbE2E1 mediated ubiquitination was reduced. The decreased level of ubiquitination was dependent on the interaction between the USP7-NTD and the UbE2E1 N-terminal extension. Furthermore, USP7 reduced the levels of polyubiquitinated UbE2E1, suggesting that UbE2E1 is a deubiquitination substrate of USP7 (Sarkari et al., 2013). Consistent with these results was the ability of USP7 to regulate the cellular stability of UbE2E1 (Sarkari et al., 2013).

1.7 Preliminary Work

Protein sequence analysis of UbE2E2 and UbE2E3 revealed that these proteins contain the USP7 binding motif P/AxxS in their N-terminal extension. Preliminary studies showed that UbE2E2 and UbE2E3 interact with the USP7-NTD via their N-terminal extensions *in vitro* (Mohamed et al, unpublished). A GST pull down was performed using wild type UbE2E proteins and GST-USP7-NTD. Figure 1.7A shows that

GST protein alone was unable to retain the UbE2E proteins suggesting that the UbE2E proteins do not bind to the GST protein. However, when the GST protein was fused with USP7-NTD, both UbE2E proteins appeared in the elution, suggesting that the UbE2E proteins interact with the USP7-NTD (Figure 1.7B). The GST pull down was repeated using mutated UbE2E proteins, in which the N-terminal extension containing the P/AxxS binding motif was deleted. The N-terminal mutants were unable to bind GST-USP7, suggesting that the UbE2E proteins interact with USP7 via their N-terminal extension (Figure 1.7C). Finally, to confirm that USP7 is interacting with the UbE2E proteins via the ^{164}DWGF^{167} motif in its NTD, a double point mutant, USP7-NTD^{DW}, in which Asp^{164} and Trp^{165} were changed to alanine residues, was used. Figure 1.7D shows that the GST-USP7-NTD^{DW} mutant did not bind to the UbE2E proteins. Together the results from Mohamed et al. (unpublished) suggest that the UbE2E proteins directly interact with the USP7-NTD *in vitro* via the P/AxxS motif in their N-terminal extension and the ^{164}DWGF^{167} motif in the USP7-NTD.

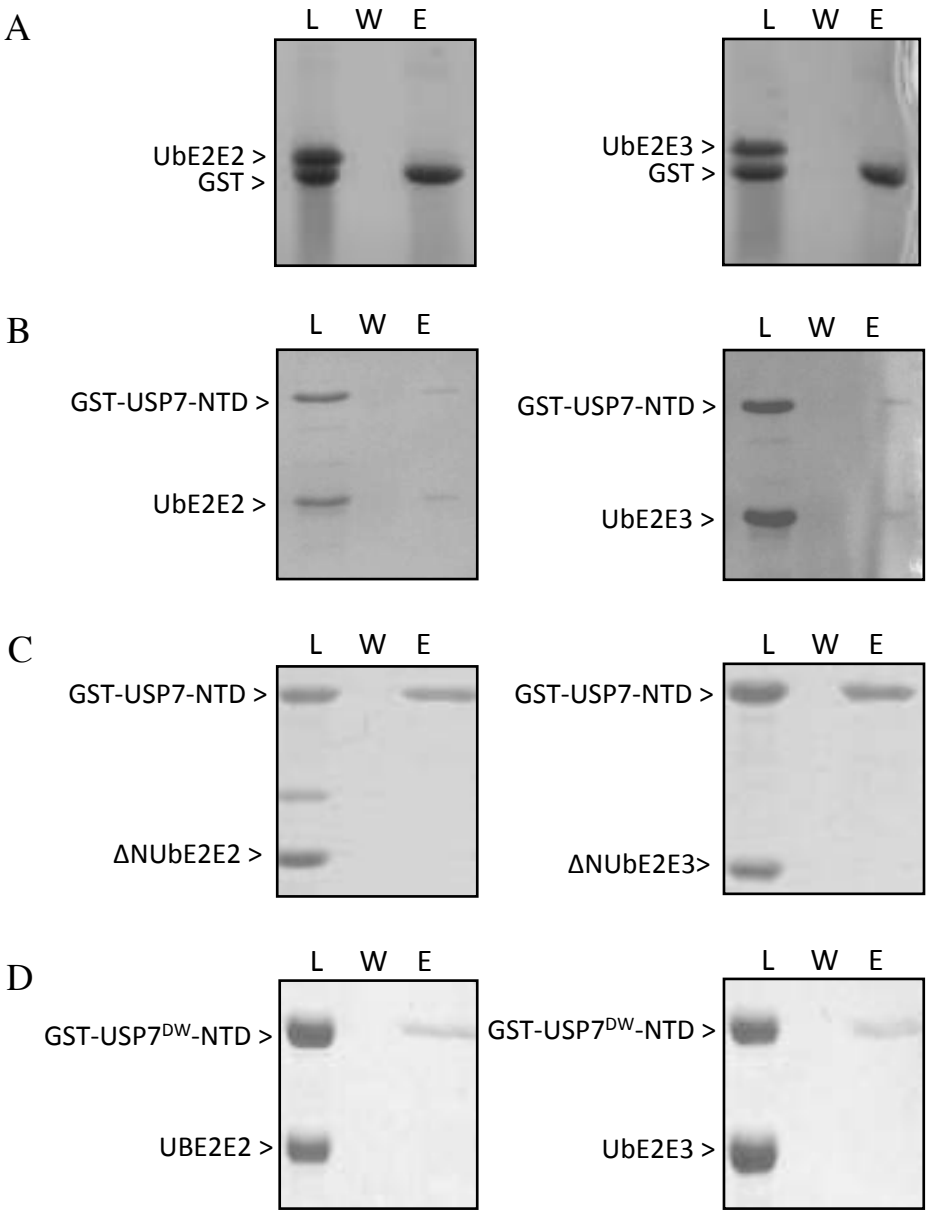

Figure 1.7: UbE2E2 and UbE2E3 interact with the USP7-NTD *in vitro* via their N-terminal extension. A GST pull-down was performed using GST-USP7-NTD and UbE2E proteins: UbE2E2 and UbE2E3. GST-USP7-NTD was incubated with the UbE2E proteins and loaded on to a glutathione resin (L). The resin was washed several times (W) and eluted using SDS-PAGE loading dye (E). GST-pull down (A) control using GST protein and wild-type UbE2E proteins (B) GST-USP7-NTD and wild-type UbE2E proteins (C) GST-USP7-NTD and a N-terminal deletion mutant of the UbE2E proteins (D) GST-USP7^{DW} and wild-type UbE2E proteins. This figure was retrieved from Mohamed et al., unpublished.

The interaction between the UbE2E proteins and the USP7-NTD was further studied using an intrinsic tryptophan fluorescence assay (Mohamed et al., unpublished). This assay used peptides corresponding to the binding motif in each of the UbE2E proteins. The dissociation constant between USP7-NTD and the respective UbE2E peptide was obtained by monitoring the change in intrinsic tryptophan fluorescence of USP7-NTD as increasing concentrations of UbE2E peptide was added. The dissociation constants revealed that each of the UbE2E proteins has a high binding affinity for USP7-NTD (Figure 1.8).

UBE2E Peptides	Dissociation Constant (Kd μM)
UBE2E1: acetyl-DSRASTSSSS-amide	9.4 ± 2.1
UBE2E2: acetyl-DDSPSTSGGS-amide	6.3 ± 1.9
UBE2E3: acetyl-DESPSTSSGS-amide	6.0 ± 2.0

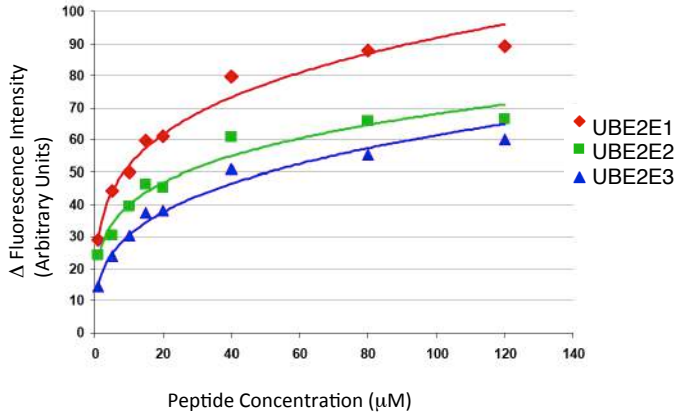

Figure 1.8: UbE2E proteins have a high binding affinity for USP7-NTD. Intrinsic tryptophan fluorescence assay showing binding affinity between UbE2E peptides and USP7-NTD. The table shows the dissociation constants between USP7-NTD and UbE2E peptides that were measured by the assay. The figure was retrieved from Mohamed et al. (unpublished).

1.8 Summary and Rationale

Previous studies have revealed that the USP7-NTD recognizes a P/AxxS motif in its substrates. A sequence analysis of the class III ubiquitin conjugating enzymes (UbE2E1, UbE2E2 and UbE2E3) revealed that these enzymes contain a conserved P/AxxS motif in their N-terminal extensions. Sarkari et al. (2013) demonstrated that UbE2E1 interacts with the USP7-NTD both *in vivo* and *in vitro*. A crystal structure of the USP7-NTD in complex with a UbE2E1 peptide revealed that the interaction occurs between the ^{8}ASTS^{11} motif in the UbE2E1 N-terminal extension and the ^{164}DWGF^{167} motif in the USP7-NTD. Through this interaction USP7 is able to deubiquitinate and salvage UbE2E1 from proteasomal degradation, thereby stabilizing cellular levels of UbE2E1 (Sarkari et al., 2013).

A preliminary study revealed that UbE2E2 and UbE2E3 directly interact with the USP7-NTD *in vitro* via their N-terminal extension. The objective of this project is threefold. First, we want to determine whether UbE2E2 and UbE2E3 interact with USP7 *in vivo*. Second, we want to determine the details of molecular interaction between UbE2E2 and the USP7-NTD, as well as, UbE2E3 and the USP7-NTD. Finally, we want to determine what effect the interaction has.

It is hypothesized that USP7 will interact with both UbE2E2 and UbE2E3 *in vivo*. We expect that the PSTS motif in the N-terminal extension of these proteins is involved in the interaction with the USP7-NTD and that the interaction is similar to what has been previously observed with other USP7-NTD substrates such as UbE2E1, p53 and Mdm2. Finally, we hypothesize that like UbE2E1, the interaction between UbE2E2 and

USP7 as well as UbE2E3 and USP7 leads to the stabilization of these proteins through USP7-mediated deubiquitination.

CHAPTER 2: MATERIALS AND METHODS

2.1 PCR Primer Synthesis

PCR primers for ube2e2 and ube2e3 were synthesized by Integrated DNA Technologies Inc. (IDT) (Toronto, Canada). The forward primers contained an *XhoI* restriction site sequence and an additional two nucleotides that were homologous to the pCMV3F-C cloning vector. The reverse primers contained the *KpnI* restriction site sequence. The sequence of the forward and reverse primers for Ube2e2 and Ube2e3 can be found in Table 2.1.

Table 2.1: PCR primer sequences for Ube2e2 and Ube2e3. The forward and reverse primers contain an *XhoI* and *KpnI* restriction site sequence, respectively.

Ube2e2	Forward	5'-GCACTCGAGCTATGTCCACTGAGGCACAAAGAG-3'
	Reverse	5'-CAGGGTACCTGTGGCGTACCGCTTGGTCCA-3'
Ube2e3	Forward	5'-GCACTCGAGCTATGTCCAGTGATAGGCAAAGGTCCG-3'
	Reverse	5'-CAGGGTACCTGTTGCGTATCTCTTGGTCCACTG-3'

*Blue – leader sequence, *Red – restriction site, *Green – bases homologous to vector, *Black – hybridization sequence

2.2 Isolation and purification of ube2e2 and ube2e3 cDNA

Ube2e2 and ube2e3 cDNA was isolated from a pET28 vector by PCR. A PCR reaction mixture was prepared on ice. Each reaction contained 1X *pfu* buffer (200mM Tris-HCl pH 8.8, 100mM $(NH_4)_2SO_4$, 2mM $MgSO_4$), 400μM dNTP mix (Fermentas Life Sciences), 1μ1 of plasmid DNA, 1μM of forward primer (IDT), 1μM of reverse primer (IDT) and 0.1μl of *pfu* DNA polymerase (purified from *E. coli*), in a total volume of

50μl. The PCR reaction was performed using Thermo Scientific® Px2 Thermal Cycler, the conditions of the PCR cycle are outlined in Table 2.2. The resulting amplified cDNA was resolved on a 1% agarose gel. The bands corresponding to the cDNA fragment of interest were excised from the gel, weighed and purified using GE Healthcare illustra™ GFX™ PCR DNA and Gel Band Purification Kit as outlined by the manufacturer. The DNA was eluted in 30μl of warm ddH_2O. The concentration of the purified cDNA was measured using Thermo Scientific® NanoDrop™ 2000.

Table 2.2: PCR cycle conditions.

STAGE 1: Denaturation (1 cycle)	95°C, 3 minutes
STAGE 2: Annealing (30 cycles)	Step 1: 95°C, 45 seconds Step 2: Annealing Temperature, 1 minute Step 3: 72°C, 5 minutes
STAGE 3: Extension (1 cycle)	72°C, 20 minutes

2.3 Isolation and purification of pCMV3F-C plasmid

The pCMV3F-C plasmid was transformed into chemically competent DH5α *E. coli* cells via heat shock transformation. The plasmid was isolated and purified using QIAGEN® QIAprep™ Spin Miniprep Kit as outlined by the manufacturer. The DNA was eluted using 50μl of warm ddH_2O. The concentration of the plasmid was measured using Thermo Scientific® NanoDrop™ 2000.

2.4 Molecular Cloning of ube2e2 and ube2e3 in to pCMV3F-C

2.4.1 Restriction Digestion

The purified ube2e inserts and pCMV3F-C plasmid were subjected to restriction digestion by *XhoI* and *KpnI*, which would cleave the DNA at the sites indicated in Figure 2.1. Each reaction contained 1μg of DNA, 1X NEBuffer 1 (New England Biolabs Inc.), 10ng of BSA, and 1μl of *Xho1* (New England Biolabs Inc.) in a final volume of 50μl. The reaction was allowed to proceed at 37°C for 1 hour. Following digestion *XhoI* was heat inactivated at 65°C for 20 minutes. *KpnI* was then added to the reaction and the reaction volume was adjusted to 60μl. The reaction was incubated at 37°C for 10 minutes. A reaction cleanup was performed following digestion using GE Healthcare illustra™ GFX™ PCR DNA and Gel Band Purification Kit. To verify digestion, the digested inserts and plasmid were resolved on a 1% agarose gel and observed by ethidium bromide staining.

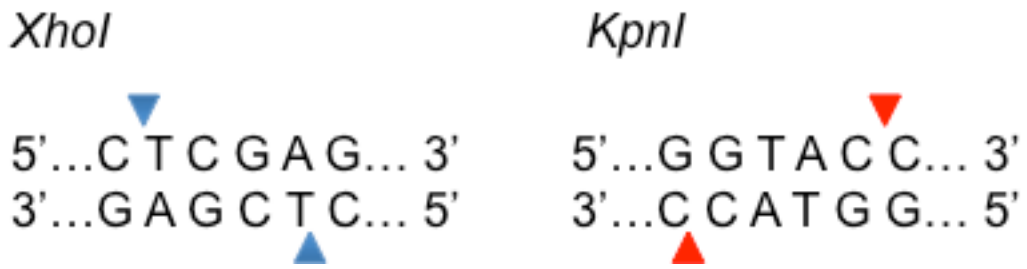

Figure 2.1: Restriction sites of *XhoI* and *KpnI*. After digestion *XhoI* creates a 5' overhang and *KpnI* creates a 3' overhang.

2.4.2 Ligation and Transformation

Digested ube2e2 and ube2e3 inserts were ligated into the digested pCMV3F-C plasmid in a 1:3 plasmid to insert molar ratio. The reaction contained 0.1μg plasmid, 0.3μg insert, 1X T4 ligase Buffer (New England Biolabs Inc.) and 400 units of T4 DNA Ligase (400 000 U/ml, New England Biolabs Inc.), in a volume of 10μl. The reaction was allowed to proceed overnight at 16°C. The resulting recombinant plasmids were transformed into chemically competent DH5α *E. coli* cells via heat shock transformation. The transformed cells were plated on to LB agar plates containing 50ng/ml kanaMycin used for selection and incubated overnight at 37°C. Of the resulting colonies, six were selected and cultured overnight at 37°C in 5ml of LB broth containing 50ng/ml kanaMycin. Plasmid DNA was isolated and purified from the resulting culture using QIAGEN® QIAprep™ Spin Miniprep Kit. The plasmid DNA was eluted using 50μl of warm ddH_2O. In order to verify successful ligation, the purified recombinant plasmids were digested with *XhoI* and *KpnI* as previously described and were resolved on a 1% agarose gel for analysis by ethidium bromide staining.

2.5 Sequencing and Sequence Analysis

Recombinant plasmids were sent to the sequencing facility at York University, Department of Biology. The sequences obtained were analyzed using NCBI Blast, ClustalW and ExPASy Translate Tool.

2.6 Cell Culture

The cell lines used in this project were Human Embryonic Kidney (HEK) 293T, Human Osteosarcoma (U2OS), Human Colon Carcinoma (HCT116) and HCT116 USP7 -/-, which were kindly provided by Dr. Bert Vogelstein (John Hopkins). Cells were kept at 37°C and 5% CO_2 in a Thermo Scientific® Forma™ Steri-Cycle™ CO_2 Incubator. U2OS and HCT116 cells were grown in McCoy's media (Wisent Bio Products) supplemented with 10% FBS and HEK293T cells were grown in DMEM media (Thermo Scientific) supplemented with 10% FBS. The cells were passaged after 48 hours.

2.7 Transfection

Cells were plated 24 hours prior to transfection in a 10 cm plate, in order to reach a confluency of 80% at the time of transfection. Thirty minutes prior to transfection, 10ml fresh growth media supplemented with 10% FBS was added to the cells. Transfection was carried out using PolyJet™ *In Vitro* DNA Transfection Reagent (SignaGen® Laboratories) using a 3:1 ratio of PolyJet™ (μl) to DNA (μg). In a microfuge tube, 10μg of plasmid DNA was mixed with 400μl of serum-free McCoy's media. In a separate microfuge tube, 30μl of PolyJet™ was mixed with 400μl of serum-free McCoy's media and immediately added to the DNA mixture. The DNA/PolyJet™ mixture was incubated for 15 minutes at room temperature and was subsequently added drop wise to the cell plate. The DNA/PolyJet™ containing media was replaced 18 hours after transfection with fresh growth media supplemented with 10% FBS. Cells were harvested for further analysis 48 hours post-transfection.

2.8 Transfection Efficiency of HCT116 USP7 -/- Cells

HCT116 USP7 -/- cells were allowed to grow in two separate 6cm dishes, each containing a glass coverslip, to 85% confluency. The cells were transfected with Green Fluorescent Protein (GFP) using either Lipofectamine® 2000 Transfection Reagent (Life Technologies) or PolyJet™ *In Vitro* DNA Transfection Reagent (SignaGen® Laboratories). Forty-eight hours post-transfection, the coverslips were removed from the plates and the cells grown on the coverslips were washed 3X with 1X PBS. Following the washes the cells were fixed in 2% paraformaldehyde in 1X PBS. The cells were then permeabilized in 0.5% Triton X-100 in 1X PBS. Cells were washed twice with PBST (PBS with 0.1% Tween 20). The nucleus was stained with Prolong® Gold Antifade Reagent with DAPI (Life Technologies) and mounted on glass microscope slides. Images were obtained using a Zeiss LSM 700 confocal microscope. The transfection efficiency was calculated by dividing the amount of GFP-positive cells by the amount of DAPI stained cells in the field of view.

2.9 Western Blotting

Whole cell extracts were resolved on 12% SDS-PAGE. The gel was electrophoresed at 70V for 30 minutes or until the bands travelled through the stacking gel and at 195V for the next 40 minutes. The proteins on the gel were transferred to a polyvinylidene difluoride (PVDF) membrane at 30V using an electrophoretic transfer cell (Biorad) overnight at 4°C. The resulting membrane was incubated in blocking buffer (5% nonfat milk in 1X PBS) for one hour at room temperature. The membrane was rinsed 3X with 1X PBS-T (recipe) and incubated with primary antibody diluted in

blocking buffer for one hour at room temperature. The membrane was washed 3X for 5 minutes with PBS-T, rinsing in between each wash. Following the washes, the membrane was incubated with horseradish peroxidase-conjugated anti-mouse antibody (1:20000 dilution in blocking buffer) or anti-rabbit antibody (1:10000 dilution in blocking buffer) for 30 minutes. The membrane was washed 3X for 15 minutes in 1X PBS-T, rinsing in between each wash. The membrane was then incubated in ECL solution (GE Healthcare) for 1 minute in dark conditions, exposed to film and developed for analysis. Western blots were quantified using ImageJ software.

2.10 Immunoprecipitations

Human Embryonic Kidney (HEK) 293T cells were co-transfected with Myc-tagged USP7 and Flag-tagged UbE2Es. Forty-eight hours post-transfection the cells were harvested and lysed using lysis buffer (50mM Tris pH 8.0, 150mM NaCl, 0.5% NP-40, 1X protease inhibitor cocktail and 1X protease inhibitor tablet (Roche)). The cells were lysed for 15 minutes at 4ºC while rotating. The cells were then sonicated using Branson Digital Sonifier® at 10% amplitude for 2 pulses (1 second on, one second off). The lysed cell were centrifuged at 17 000 xg for 10 minutes at 4ºC. The concentration of the cell lysate was quantified using a Bradford protein assay (Bioshop). Cells used for the control experiment were co-transfected with an empty vector and Myc-tagged USP7.

2.10.1 Immunoprecipitation of Flag-UBE2Es

Forty microliters of anti-Flag M2 affinity gel beads (Sigma, A2220) were pre-washed three times with 0.5ml of 1X PBS. One milligram of total cell lysate was incubated with the pre-washed beads, overnight at 4°C. The immunoprecipitated complex was washed four times with lysis buffer (50mM Tris pH 8.0, 150mM NaCl, 0.5% NP-40) and was eluted by boiling in 5X SDS loading dye. The elution was resolved on 12% SDS-PAGE followed by immunoblotting with antibodies against Myc-tag (Abcam, ab9106) and Flag-tag (Sigma, F3165). Cells co-transfected with empty pCMV3F-C vector and Myc-tagged USP7 were used as a negative control.

2.10.2 Immunoprecipitation of Myc-USP7

Cell lysate obtained from a single batch of cells was divided into two microfuge tubes, each containing one milligram of total cell lysate. The cell lysate was pre-cleared with Protein A/G PLUS Agarose (Santa Cruz, sc-2003) for 30 minutes at 4°C. The pre-cleared lysate was incubated with 2μg of Myc tag antibody (Abcam, ab9106) or 2μg of normal rabbit IgG (Santa Cruz, sc-2027) overnight at 4°C. Following incubation, 30μl of Protein A/G PLUS Agarose (Santa Cruz, sc-2003) was added to the lysates and incubated for 1 hour at 4°C. The immunoprecipitated complex was washed 4X with lysis buffer (50mM Tris pH 8.0, 150mM NaCl, 0.5% NP-40) and was eluted by boiling in 5X SDS loading dye. The elution was resolved on 12% SDS-PAGE followed by immunoblotting with antibodies against Myc-tag and Flag-tag (Sigma, F3165).

2.11 Synthesis of UbE2E2 and UbE2E3 Peptides

The UbE2E2 and UbE2E3 peptides used for crystallization were synthesized by CanPeptide Inc. (Montreal, Canada). In order to mimic natural peptides, the peptides were acetylated at the N-terminal end and amidated at the C-terminal end. Peptides were dissolved in crystallization buffer prior to use.

2.12 Crystallization of USP7-NTD:UbE2E2 and USP7-NTD:UbE2E3

2.12.1 Purification of USP7-NTD

USP7-NTD was purified by Niharika Luthra, York University. USP7-NTD was purified using Ni^{2+} Affinity Chromatography and eluted in a buffer containing 100mM

Hepes pH 7.5, 500mM NaCl, 10% glycerol, 250mM Imidazole and 0.5mM TCEP. Thrombin was used to remove the 6X His-tag from the purified USP7-NTD. The His-cleaved USP7-NTD was subjected to size exclusion chromatography in order to remove impurities and exchange the buffer to 20mM Hepes pH 7.5, 500mM NaCl. The cleaved protein was used for co-crystal trials.

2.12.2 Co-Crystallization of USP7-NTD with UbE2E Peptides

Purified USP7-NTD was concentrated to 100mg/ml and mixed with 5-fold molar excess of peptide for either UbE2E2 (^{9}DDSPSTSGGS^{18}) or UbE2E3 (^{10}DESPSTSSGS^{19}). In order to allow complex formation, the mixture was incubated overnight at 4ºC. Following incubation, co-crystal trials were set up for the USP7-NTD:UbE2E^{PSTS} complex using USP7-NTD:HdmX as microseeds. 1μl of protein complex was mixed with 0.25μl of USP7-NTD:HdmX as microseed and 0.75μl crystallization buffer (30% PEG 4000, 0.1M Tris pH 8.5 and 0.2M Lithium Sulfate). The resulting 2μl mixture was sealed in a chamber using the hanging drop method. The sealed chamber was incubated at 4ºC in dark conditions.

2.12.3 Data Collection and Structure Determination

The USP7-NTD:UbE2E2 ^{PSTS} and USP7-NTD:UbE2E3 ^{PSTS} crystals were flash frozen. X-ray data from the frozen crystals was collected at 100K on a Rigaku MicroMax007 rotating anode diffractometer with a 944+ CCD detector. HKL-2000

software was used to integrate and scale the data. The molecular replacement component in CNS (version 1.3) was used to determine the structure using USP7-NTD (PDB ID 1YY6) without peptide as the search model. CNS 1.3 was also used for picking water molecules and for refinement of torsion angles and B-factors. The program Coot was used for electron density visualization, model building and model rebuilding (after inspecting $2F_o$-F_c and F_o-F_c maps). Figures were created using PyMol.

2.13 UbE2E2 Turnover Assay in HCT116 Cells

HCT116 WT and HCT116 USP7 -/- cells were grown in 6cm dishes to 75% confluency. The cells were treated with 50μg/ml of cycloheximide (Sigma, C4859) diluted in complete media. The cells were harvested 0, 2, 4, 8, 24 and 48 hours post-treatment. Cells were lysed with lysis buffer (50mM Tris pH 8.0, 150mM NaCl, 0.5% NP-40, 1X protease inhibitor cocktail and 1X protease inhibitor tablet (Roche)). Lysis was allowed to proceed for 15 minutes at 4ºC, while rocking followed by sonication using Branson Digital Sonifier® at 10% amplitude and 2 pulses (1 second on, 1 second off). The cell lysate was then centrifuged at 17 000 xg at 4ºC. Fifty micrograms of total cell lysate was resolved on 12% SDS-PAGE and immunoblotted with antibodies against USP7 (Bethyl, A300-033A), UbE2E2 (Bethyl, A303-485A) and GAPDH (Santa Cruz, 0411).

2.14 USP7 Rescue Assay in HCT116 USP7 -/- Cells

HCT116 USP7 -/- cells were grown in 6cm plates to 75% confluency. The cells were transfected with empty vector, Myc-USP7-WT, Myc-USP7-C223S and Myc-USP7-DW (USP7 plasmids provided by Rahima Khutan, York University). The cells were harvested 48 hours post-transfection. Harvested cells were lysed with lysis buffer (50mM Tris pH 8.0, 150mM NaCl, 0.5% NP-40, 1X protease inhibitor cocktail and 1X protease inhibitor tablet (Roche)). Lysis was allowed to proceed for 15 minutes at 4ºC, while rocking followed by sonication using Branson Digital Sonifier® at 10% amplitude and 2 pulses (1 second on, 1 second off). The cell lysate was then centrifuged at 17 000 xg at 4ºC. Fifty micrograms of total cell lysate was resolved on 12 % SDS-PAGE and immunoblotted with antibodies against USP7 (Bethyl, A300-033A), UbE2E2 (Bethyl, A303-485A) and GAPDH (Santa Cruz, 0411).

CHAPTER 3: RESULTS

3.1 USP7-NTD Interacts with UbE2E2 and UbE2E3 *In Vivo*

A previous study revealed that UbE2E2 and UbE2E3 interact with the USP7-NTD *in vitro*, via their N-terminal extension (Mohamed et al., unpublished). To determine whether these proteins interact *in vivo,* a co-immunoprecipitation assay was performed. HEK293T cells were co-transfected with Myc-tagged USP7 and Flag-tagged UbE2E2. The cells were subjected to co-immunoprecipitation using an antibody targeted against the Myc-tag. An IgG antibody was used as a negative control to ensure that the interacting protein, in this case Flag-UbE2E2, is binding to myc-USP7 and not the IgG antibody. The resulting immunoprecipitated complex was observed using an immunoblot. Figure 3.1A shows that Flag-UbE2E2 was detected in the immunoprecipitated complex of Myc-USP7 but not IgG alone.

To further validate these results, we performed the reciprocal of this experiment, where the co-transfected cells were subjected to co-immunoprecipitation using an anti-Flag antibody. Cells co-transfected with an empty pMCV3F-C vector were used as a negative control. Myc-USP7 was observed in the immunoprecipitated complex of Flag-UbE2E2 but not in the immunoprecipitated complex of cells co-transfected with an empty vector and Myc-USP7 (Figure 3.1B).

The same sets of experiments were repeated for cells co-transfected with Myc-tagged USP7 and Flag-tagged UbE2E3. Flag-UbE2E3 was observed in the immunoprecipitated complex of Myc-USP7 but not IgG alone (Figure 3.2A). Furthermore, Myc-USP7 was observed in the immunoprecipitated complex of

Flag-UbE2E3 and not in cells transfected with empty vector (Figure 3.2B). Together, these results suggest that USP7 interacts with UbE2E2 and UbE2E3 *in vivo*.

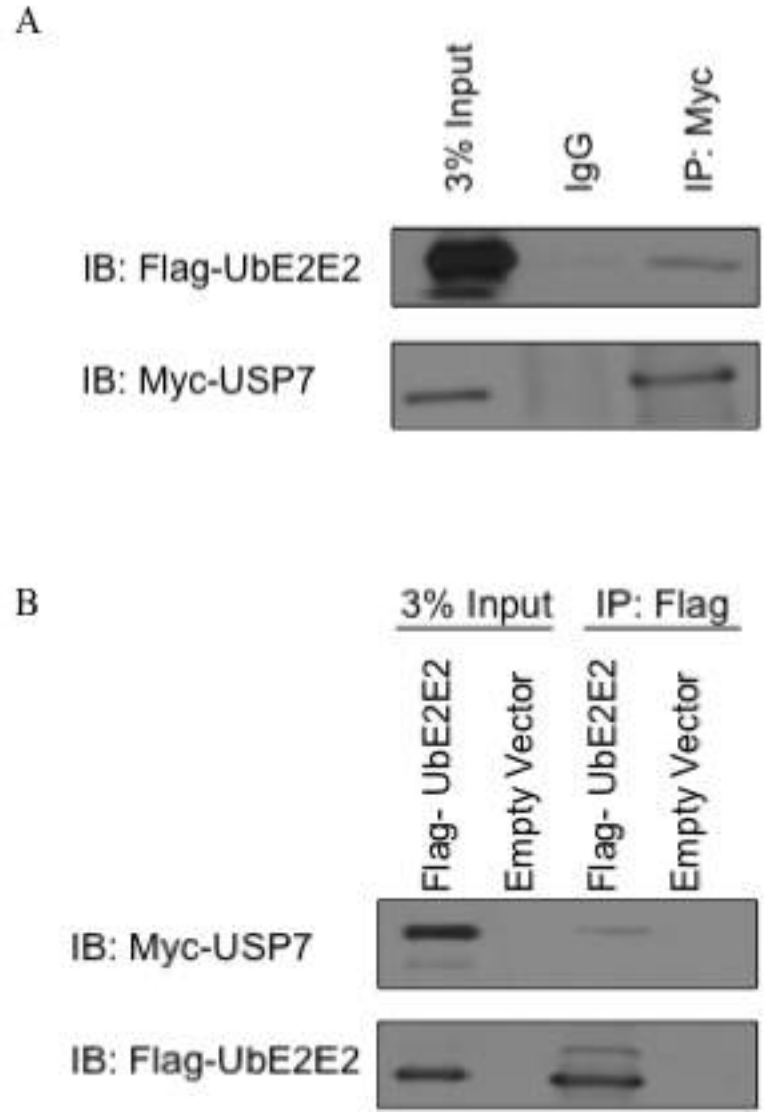

Figure 3.1: USP7 interacts with UbE2E2 *in vivo*. (A) 293T cells were co-transfected with Myc-USP7 and Flag-UbE2E2. Twenty-four hours post transfection whole cell extracts were subjected to immunoprecipitation using anti-Myc and rabbit IgG antibodies. The immunoprecipitated complex was immunoblotted using anti-Flag and anti-Myc antibodies. The input for both IP:Myc and IP:IgG came from the same cell extract. Thirty micrograms of whole cell extract was used as input. (B) 293T cells were co-transfected with Myc-USP7 and Flag-UbE2E2. For control purposes 293T cells were transfected with empty pCMV3F-C vector. Twenty-four hours post-transfection whole cell extracts were subjected to immunoprecipitation using anti-Flag M2 affinity gel. The immunoprecipitated complex was immunoblotted using anti-Myc and anti-Flag antibodies. Thirty micrograms of whole cell extract was used as input.

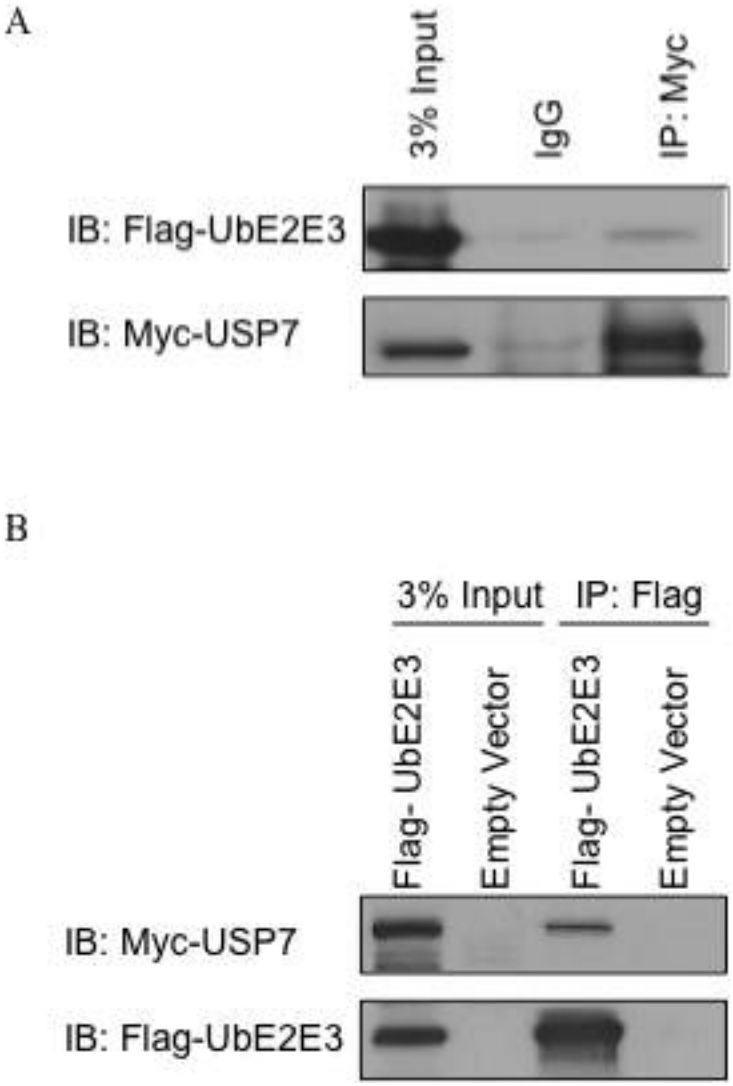

Figure 3.2: USP7 interacts with UbE2E3 *in vivo*. (A) 293T cells were co-transfected with Myc-USP7 and Flag-UbE2E3. Twenty-four hours post transfection whole cell extracts were subjected to immunoprecipitation using anti-Myc and rabbit IgG antibodies. The immunoprecipitated complex was immunoblotted using anti-Flag and anti-Myc antibodies. The input for both IP:Myc and IP:IgG came from the same cell extract. Thirty micrograms of whole cell extract was used as input. (B) 293T cells were co-transfected with Myc-USP7 and Flag-UbE2E3. For control purposes 293T cells were transfected with empty pCMV3F-C vector. Twenty-four hours post-transfection whole cell extracts were subjected to immunoprecipitation using anti-Flag M2 affinity gel. The immunoprecipitated complex was immunoblotted using anti-Myc and anti-Flag antibodies. Thirty micrograms of whole cell extract was used as input.

3.2 Molecular Analysis of the Interaction Between USP7:UbE2E2 and USP7:UbE2E3

3.2.1 Crystallization and Structure Determination of USP7:UbE2E2 and USP7:UbE2E3

In order to gain insight on the molecular basis of interaction between USP7-NTD and UbE2E2, as well as USP7-NTD and UbE2E3, we synthesized peptides corresponding to the interaction motif in the UbE2E2 (^{9}DDSPSTSGGS^{18}) and UbE2E3 (^{10}DESPSTSSGS^{19}) N-terminal extensions. The peptides were co-crystallized with the USP7-NTD, which was purified using Ni^{2+} affinity chromatography. The crystals grew at 4ºC in dark conditions after one week in a buffer containing 30% PEG 4000, 0.1M Tris pH 8.5 and 0.2M lithium sulfate. The protein complexes formed between USP7-NTD:UbE2E2^{12}PSTS^{15} (USP7:UbE2E2^{PSTS}) and USP7-NTD:UbE2E3^{13}PSTS^{16} (USP7:UbE2E3^{PSTS}) formed crystals that are rod-shaped. Figure 3.3 shows the rod-shaped crystals formed by the USP7:UbE2E3^{PSTS} complex. The crystals were frozen and exposed to X-rays, producing a unique diffraction pattern. Figure 3.4 shows the diffraction pattern produced for the USP7:UbE2E3^{PSTS} complex. Figure 3.4A shows reflections at lower resolutions; reflections are clearly observed until the 2.99Å resolution shell. A magnified image of the higher resolution shells shows reflections in the 2.11Å resolution shell (Figure 3.4B).

The crystal structures of USP7-NTD:UbE2E2^{PSTS} and USP7-NTD:UbE2E3^{PSTS} were determined using molecular replacement to a resolution of 1.75Å and 2.00Å, respectively (Table 3.1). The structure of USP7-NTD:UbE2E2^{PSTS} was refined to an R_{work} of 0.198 and an R_{free} of 0.215 with 126 water molecules (Table 3.1). The

structure for USP7:UbE2E3^{PSTS} was refined to an R_{work} of 0.207 and an R_{free} of 0.240 with 175 water molecules (Table 3.1). The Ramachandran Plot for both USP7:UbE2E2^{PSTS} and USP7:UbE2E3^{PSTS} indicates that 95.6% of the residues were in their most favored spot.

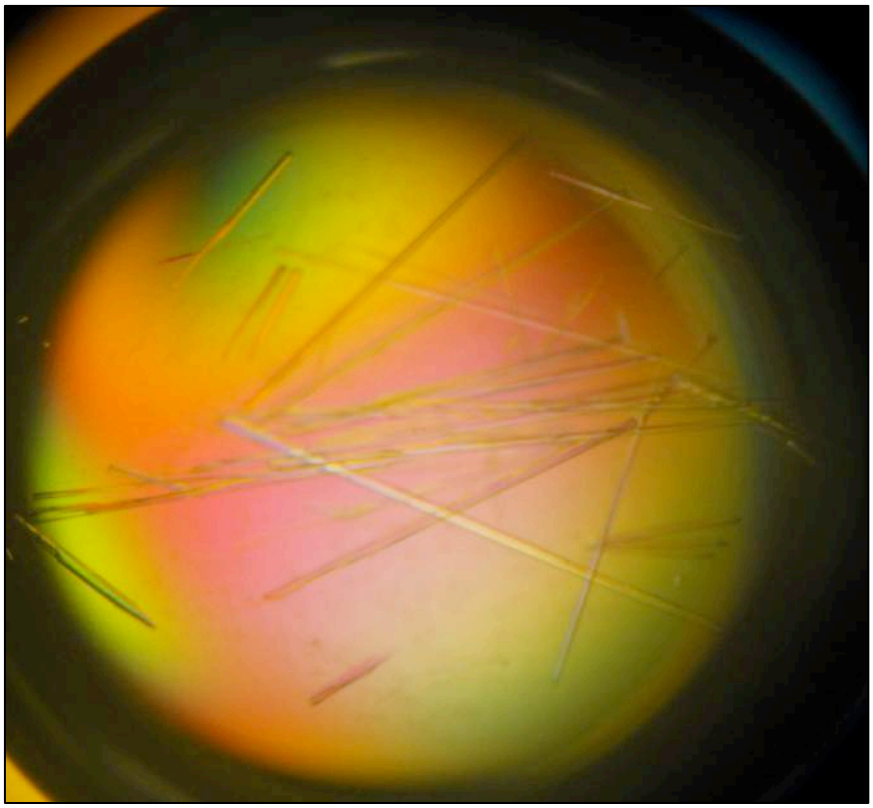

Figure 3.3: UbE2E3^{13}PSTS^{16} co-crystalized with USP7-NTD forming long, rod-shaped crystals. 100 mg/ml of purified USP7-NTD was incubated with 5-fold molar excess of UbE2E3 peptide ^{10}DESPSTSSGS^{19}, overnight at 4°C. Co-crystal trials were set up using USP7-NTD:HdmX as a microseed and a crystallization buffer containing 30% PEG 4000, 0.1M Tris pH 8.5 and 0.2M Lithium Sulfate. Crystals grew in dark conditions at 4°C over a one week period. The crystals obtained were long and rod-shaped.

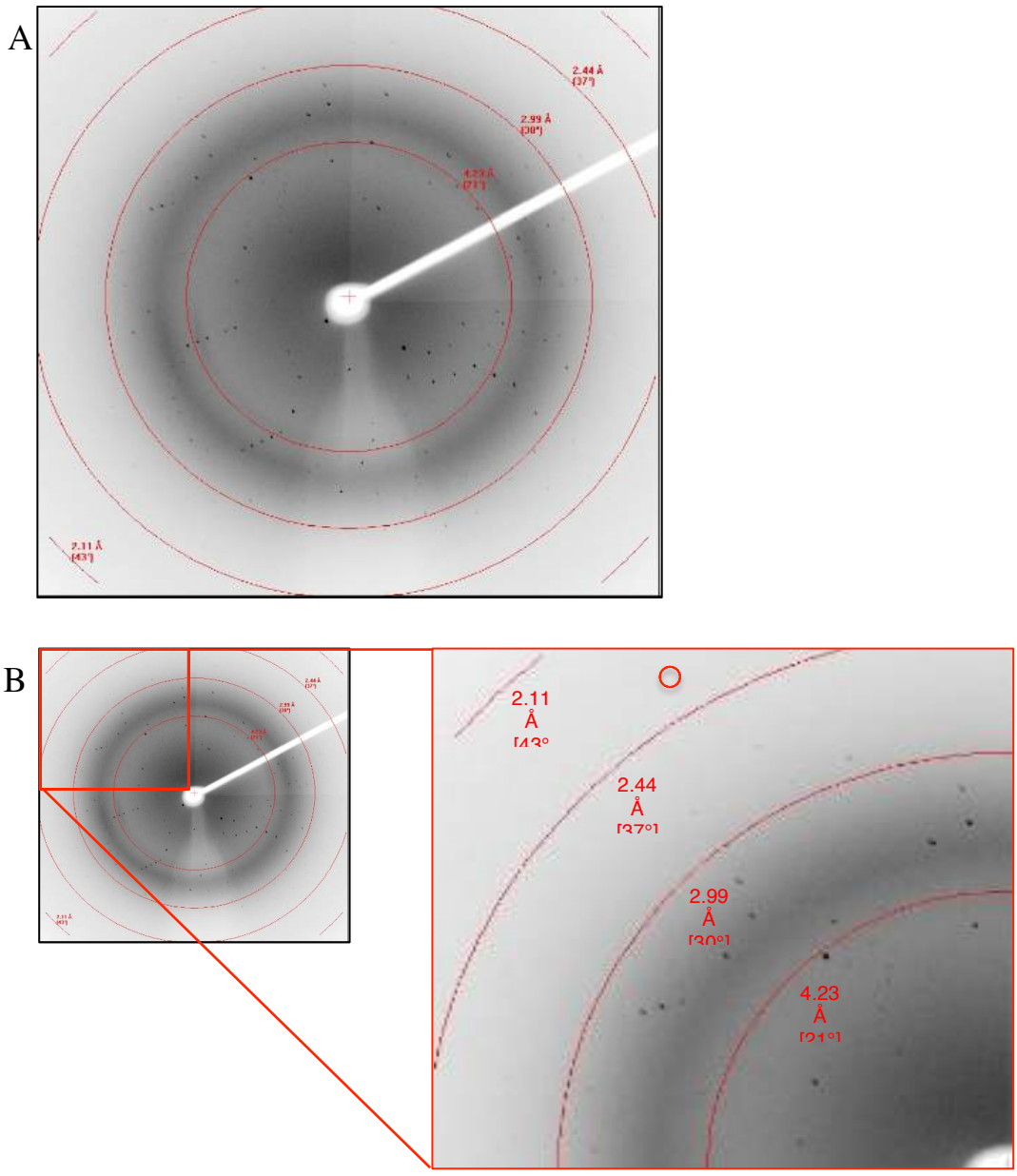

Figure 3.4: X-ray diffraction pattern from a USP7:UbE2E3^{PSTS} co-crystal. X-ray data was collected at 100K on a Rigaku MicroMax007 rotating anode diffractometer with a 944+ CCD detector using a frozen protein crystal. When an X-ray beam strikes the protein crystal, it produces a pattern of spots called reflections on a detector. The relative intensity and position of the reflections can be used to determine the arrangement of molecules within the crystal. (A) An image of the resulting diffraction pattern showing reflections in all resolution shells. (B) Magnified image showing reflections in higher resolution shells. Some reflections are circled red.

Table 3.1: X-ray data collection and refinement parameters for USP7:UbE2E2^{PSTS} and USP7:UbE2E3^{PSTS}

X-Ray Data	UbE2E2 (^{9}DDSPSTSGGS^{18})	UbE2E3 (^{10}DESPSTSSGS^{19})
Space Group	$P4_1$	$P4_1$
Resolution (Å)	50.0 – 1.75	50.0 – 2.00
Unit Cell Axis (Å^3)	69.9 x 69.9 x 45.7	70.0 x 70.0 x 46.0
Molecules/AU	1	1
Total Observations (#)	132 400	108 466
Unique Reflections (#)	21738	14 277
Intensity (I / σ<I>)	20.1 (2.1)	12.8 (2.8)
Completeness (%)	96.8 (74.7)	93.6 (88.8)
$^{a}R_{sym}$	0.063 (0.570)	0.083 (0.337)
Refinement		
R_{work}	0.198	0.207
R_{free}	0.215	0.240
Protein Atoms (#)	1160	1362
Water Molecules (#)	126	175
rmsd bonds (Å)	0.005	0.006
rmsd angles (°)	1.4	1.4
rmsd dihedrals (°)	25.3	25.5
rmsd improper (°)	0.87	0.83
Thermal factors (Å^2)	17.0	19.6
Ramachandran Plot		
Most Favoured	0.956	0.956
Additionally allowed	0.037	0.044

Numbers in brackets refer to the highest resolution shell, 1.78 Å to 1.75 Å for the USP7:UbE2E2^{PSTS} data and 2.08 to 2.00 Å for the USP7:UbE2E3^{PSTS} data. $^{a}R_{sym} = \Sigma |I-<I>| / \Sigma I$ where I is the observed intensity and <I> is the average intensity from multiple observations of symmetry-related reflections.

3.2.2 UbE2E2 and UbE2E3 Bind the β7-strand of the USP7-NTD

The molecular structure of USP7-NTD and UbE2E2^{12}PSTS^{15} is displayed in Figure 3.5A with the USP7-NTD displayed in violet and the UbE2E2^{12}PSTS^{15} peptide displayed in green. In this model, the USP7-NTD begins at residue 63 instead of 54 because the initial residues are too disordered to assign their atomic structure. Furthermore, the UbE2E2 peptide, ^{9}DDSPSTSGGS^{18}, has been modeled from residues 12-15. The structure of the USP7-NTD has been previously described as an anti-parallel β-sandwich comprising of eight anti-parallel β-strands. Figure 3.5A shows that the UbE2E2 peptide binds the β7 strand of the USP7-NTD. A side view of the protein complex shows that the UbE2E2 peptide hugs the β7 strand and makes contacts with two additional β strands along its length (Figure 3.5B). Figures 3.5C and 3.5D depict a surface diagram and an electrostatic diagram, respectively, of USP7-NTD bound to the UbE2E2 peptide.

The molecular structure of USP7-NTD and UbE2E3^{13}PSTS^{16} is displayed in Figure 3.6A with USP7-NTD displayed in blue and the UbE2E3^{13}PSTS^{16} peptide displayed in yellow. Like in the USP7-NTD:UbE2E2^{12}PSTS^{15} structure, the USP7-NTD is modeled from residue 63 instead of 54. The UbE2E3 peptide, ^{10}DESPSTSSGS^{19}, is modeled from residues 11-16. The UbE2E3 peptide binds the β7 strand of the USP7-NTD (Figure 3.6A). Like the UbE2E2 peptide, the UbE2E3 peptide hugs the β7 and contacts two additional β strands along its length (Figure 3.6B). Figure 3.6C and Figure 3.6D show a surface and electrostatic diagram, respectively, of the USP7-NTD bound to the UbE2E3 peptide.

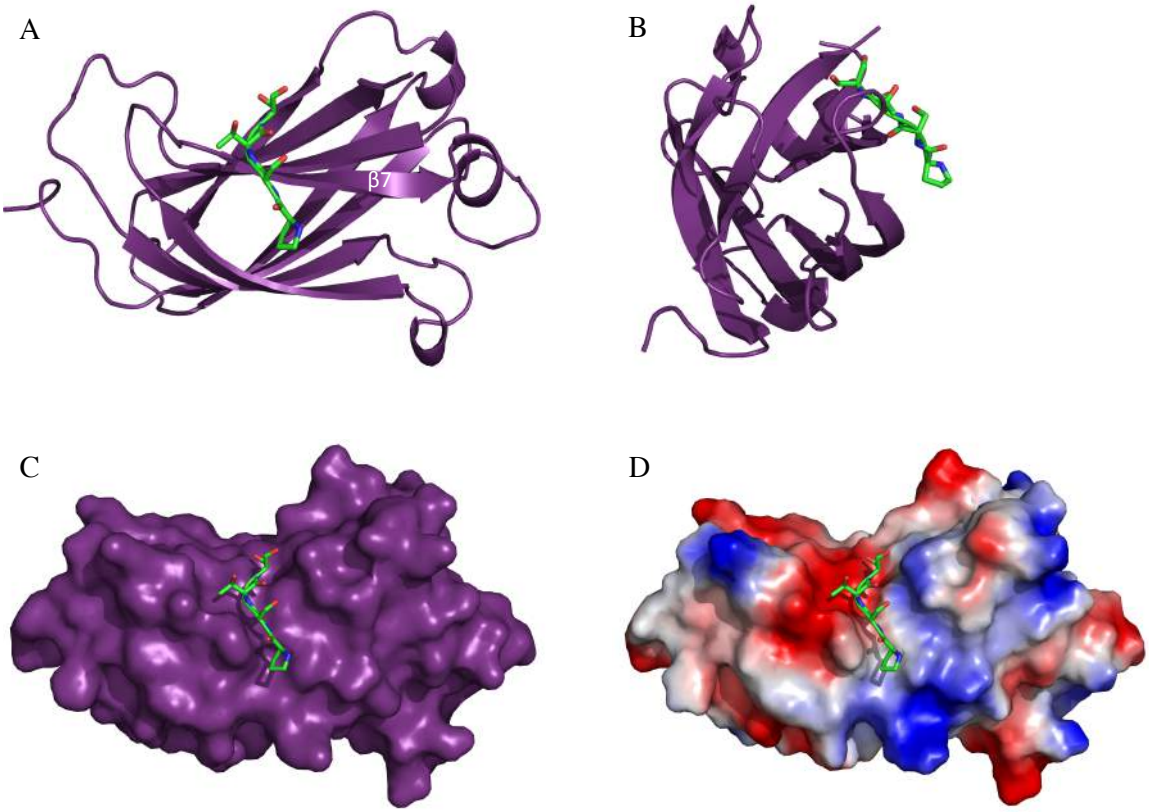

Figure 3.5: The crystal structure of USP7-NTD binding to UbE2E2^{12}PSTS^{15} reveals that UbE2E2 binds USP7 at β-strand β7. (A) Cartoon representation of USP7-NTD (violet) binding to the UbE2E2^{12}PSTS^{15} peptide (green). The structure reveals that UbE2E2 binds the β7 strand of USP7. (B) A side representation of the UbE2E2 peptide (green) binding the USP7-NTD (violet) showing that the peptide hugs the β7 strand of USP7. (C) A surface and (D) electrostatic representation of UbE2E2^{12}PSTS^{15} binding to USP7-NTD.

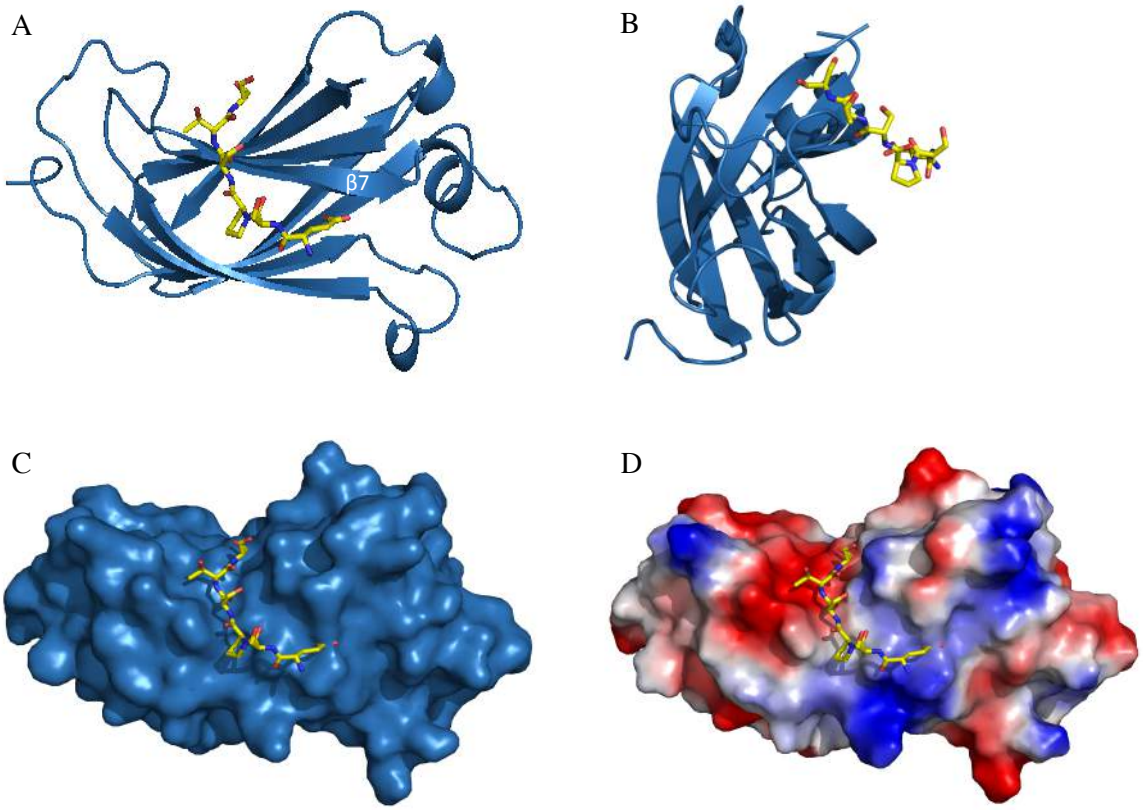

Figure 3.6: The crystal structure of USP7-NTD binding to UbE2E3^{13}PSTS^{16} reveals that UbE2E3 binds USP7 at β-strand β7. (A) Cartoon representation of USP7-NTD (blue) binding to the UbE2E3^{13}PSTS^{16} peptide (yellow). The structure reveals that UbE2E3 binds the β7 strand of USP7. (B) A side representation of the UbE2E3 peptide (yellow) binding the USP7-NTD (blue) showing that the peptide hugs the β7 strand of USP7. (C) A surface and (D) electrostatic representation of UbE2E3^{13}PSTS^{16} binding to USP7-NTD.

3.2.3 UbE2E2 and UbE2E3 sit in a shallow groove on the surface of the USP7-NTD when binding to the β7 strand

Figure 3.7A and 3.7C depict cartoon and surface diagrams, respectively, of the USP7-NTD (violet) bound to the UbE2E2 peptide (green). It is evident from these figures that the UbE2E2 peptide sits in a shallow groove on the surface of the USP7-NTD. When Figure 3.7A is rotated 45 degrees, it can be seen that the β7 strand of the USP7-NTD makes up part of the shallow groove (Figure 3.7B). Figure 3.7C, when rotated 45 degrees, shows that the UbE2E2 peptide perfectly fits into the shallow groove on the surface of the USP7-NTD (Figure 3.7D).

Identical observations were made for the interaction between the USP7-NTD (blue) and the UbE2E3 peptide (yellow) (Figure 3.8). Figure 3.8A and Figure 3.8C show that the UbE2E3 peptide binds the USP7-NTD at the shallow groove. The shallow groove contains the β7 strand of the USP7-NTD, which binds the UbE2E3 peptide (Figure 3.8B). The UbE2E3 peptide sits perfectly in the shallow groove on the surface of the USP7-NTD (Figure 3.8D).

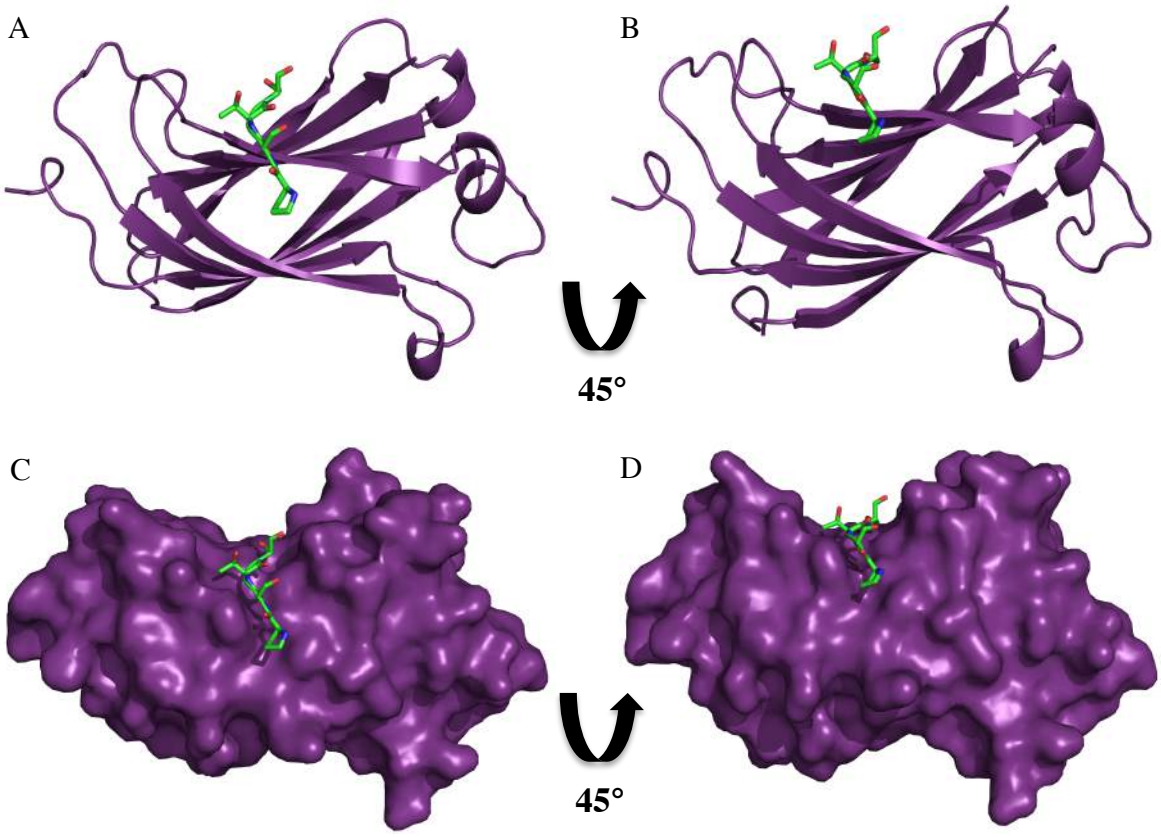

Figure 3.7: UbE2E2^{12}PSTS^{15} binds the shallow groove on the surface of USP7-NTD containing the β7 strand residues ^{164}DWGF^{167}. (A) A cartoon representation of the UbE2E2^{12}PSTS^{15} peptide (green) binding USP7-NTD (violet) (B) rotated 45° showing that the UbE2E2^{12}PSTS^{15} peptide binds in the shallow groove of USP7-NTD containing the β7 strand residues ^{164}DWGF^{167}. (C) Surface representation of the UbE2E2^{12}PSTS^{15} peptide (green) binding USP7-NTD (violet) (D) rotated 45° showing that the UbE2E2^{12}PSTS^{15} peptide binds in the shallow groove of USP7-NTD containing the β7 strand residues ^{164}DWGF^{167}.

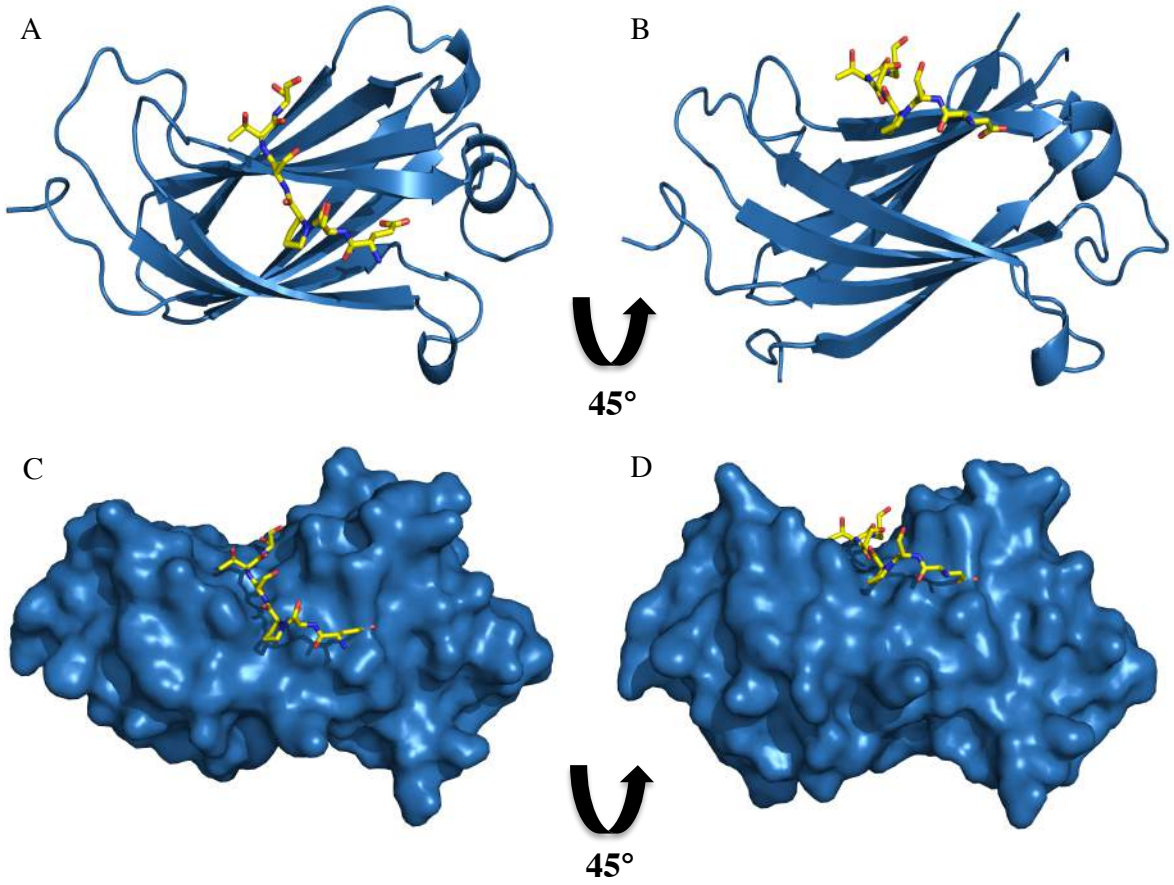

Figure 3.8: UbE2E3^{13}PSTS^{16} binds the USP7-NTD at the shallow groove containing the β7 strand residues ^{164}DWGF^{167}. (A) A cartoon representation of the UbE2E3^{13}PSTS^{16} peptide (yellow) binding USP7-NTD (blue) (B) rotated 45° showing that the UbE2E3^{13}PSTS^{16} peptide binds in the shallow groove of USP7-NTD containing the β7 strand residues ^{164}DWGF^{167}. (C) Surface representation of the UbE2E3^{13}PSTS^{16} peptide (yellow) binding USP7-NTD (blue) (D) rotated 45° showing that the UbE2E3^{13}PSTS^{16} peptide binds in the shallow groove of USP7-NTD containing the β7 strand residues ^{164}DWGF^{167}.

3.2.4 UbE2E2 and UbE2E3 Make Several Contacts with the USP7-NTD

The UbE2E2^{12}PSTS^{15} and the UbE2E3^{13}PSTS^{16} peptides form several interactions with the β7-strand of the USP7-NTD. Pro12 of UbE2E2 and Pro13 of UbE2E3 form Van der Waals interactions with USP7 Trp165 and Phe167 (Figure 3.9 B; Figure 3.10B). The side chain hydroxyl of UbE2E2 Ser13 and UbE2E3 Ser14 forms a water-mediated hydrogen bond with the main-chain amide of USP7 Ser168 (Figure 3.9C; Figure 3.10C). The main-chain amide and carbonyl groups of UbE2E2 Ser13 and UbE2E3 Ser14 interact with the main-chain amide and carbonyl groups of USP7 Gly166 (Figure 3.9C; Figure 3.10C). UbE2E2 Thr14 and UbE2E3 Thr15 do not make any interactions with the USP7-NTD (Figure 3.9B; Figure 3.10B). The side-chain hydroxyl of UbE2E2 Ser15 and UbE2E3 Ser16 forms hydrogen bonds with the main and side chain of USP7 Asp164 (Figure 3.9D)

The crystal structure of another class III ubiquitin-conjugating enzyme, UbE2E1, in complex with the USP7–NTD, was recently determined (Sarkari et al., 2013). UbE2E1 has an ASTS motif in its N-terminal extension, whereas UbE2E2 and UbE2E3 have a PSTS motif. The peptide for UbE2E1 and UbE2E2 are shown in Figure 3.11A and Figure 3.11B. An overlay of the peptides shows that all residues are completely aligned, indicating that they have a conserved interaction with the USP7-NTD (Figure 3.11C; Figure 3.12C). When the overlay is rotated 180 degrees, the difference of Pro12 in UbE2E2 and Ala8 in UbE2E1 can be seen. Although the residues are different, they align perfectly (Figure 3.11D). The same observations were made when comparing the UbE2E1 peptide to that UbE2E3 in Figure 3.12.

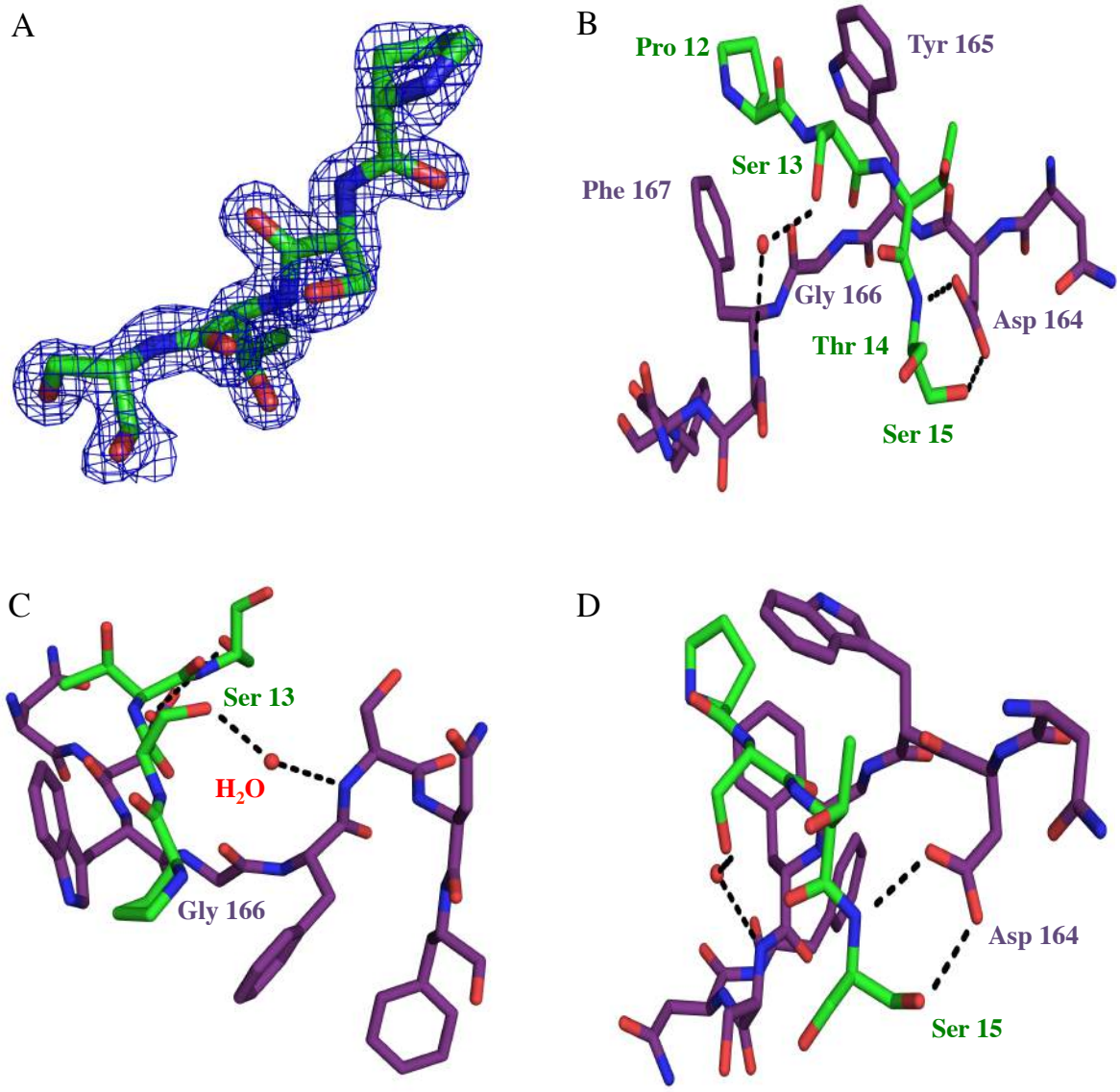

Figure 3.9: Molecular details of interaction between USP7-NTD and UbE2E2^{12}PSTS^{15} peptide. (A) A $2F_oF_c$ electron density map showing that UbE2E2^{12}PSTS^{15} at 1 σ. (B) Molecular details of interaction between USP7-NTD (violet) and UbE2E2^{12}PSTS^{15} (green) are shown in stick format. Important residues for interaction are labeled. Black dashed lines represent hydrogen bonds. (C) A closer view of the hydrogen bond between Ser13 in UbE2E2, a water molecule and the main chain in USP7-NTD (D) A closer view of the hydrogen bond between Asp164 in USP7-NTD and Ser15 in UbE2E2.

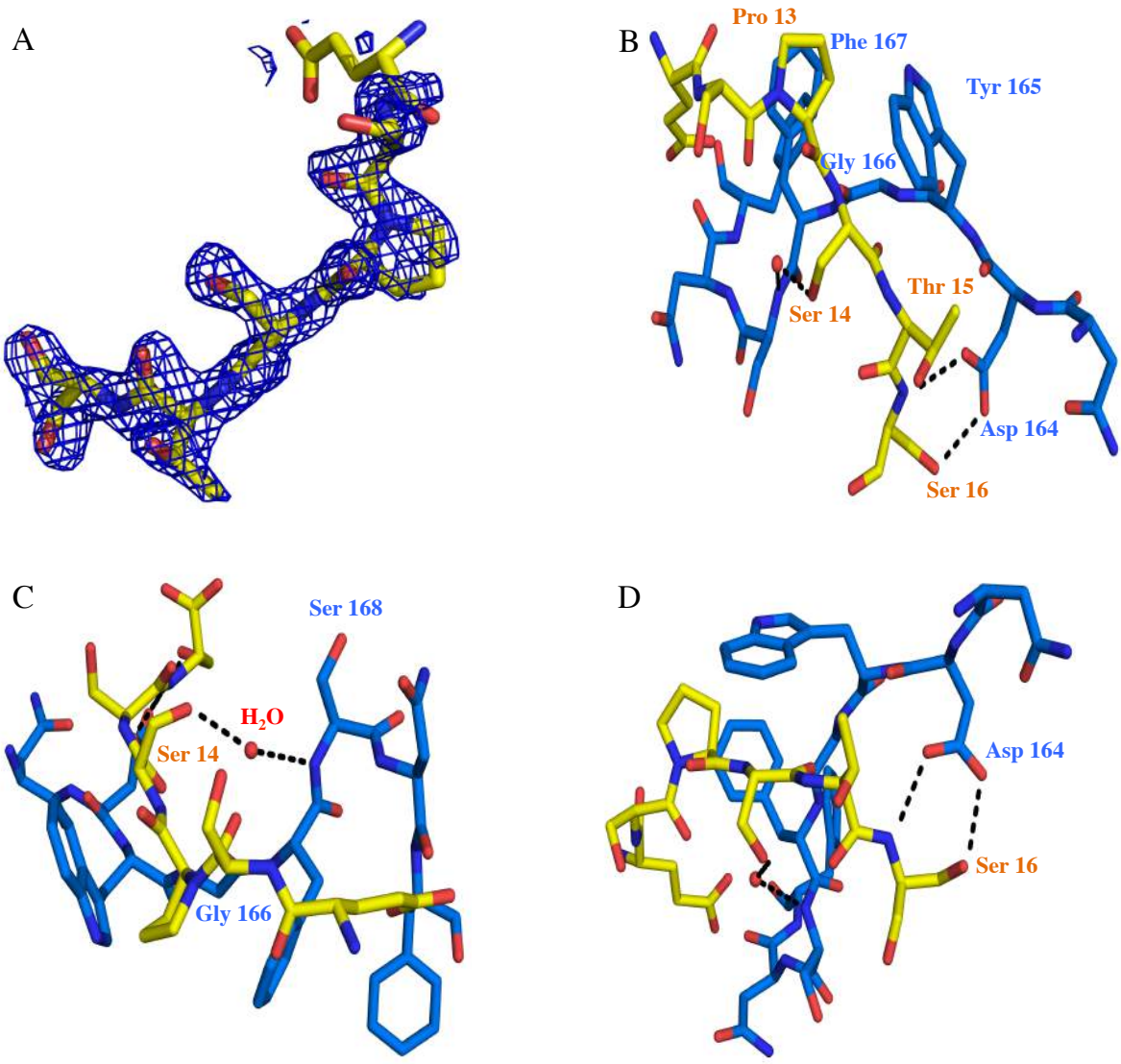

Figure 3.10: Molecular details of interaction between USP7-NTD and UbE2E3^{13}PSTS^{16} peptide. (A) A $2F_oF_c$ electron density map showing that UbE2E3^{13}PSTS^{16} at 1 σ. (B) Molecular details of interaction between USP7-NTD (blue) and UbE2E3^{13}PSTS^{16} (yellow) are shown in stick format. Important residues for interaction are labeled. Black dashed lines represent hydrogen bonds. (C) A closer view of the hydrogen bond between Ser14 in UbE2E3, a water molecule and the main chain in USP7-NTD (D) A closer view of the hydrogen bond between Asp164 in USP7-NTD and Ser16 in UbE2E3.

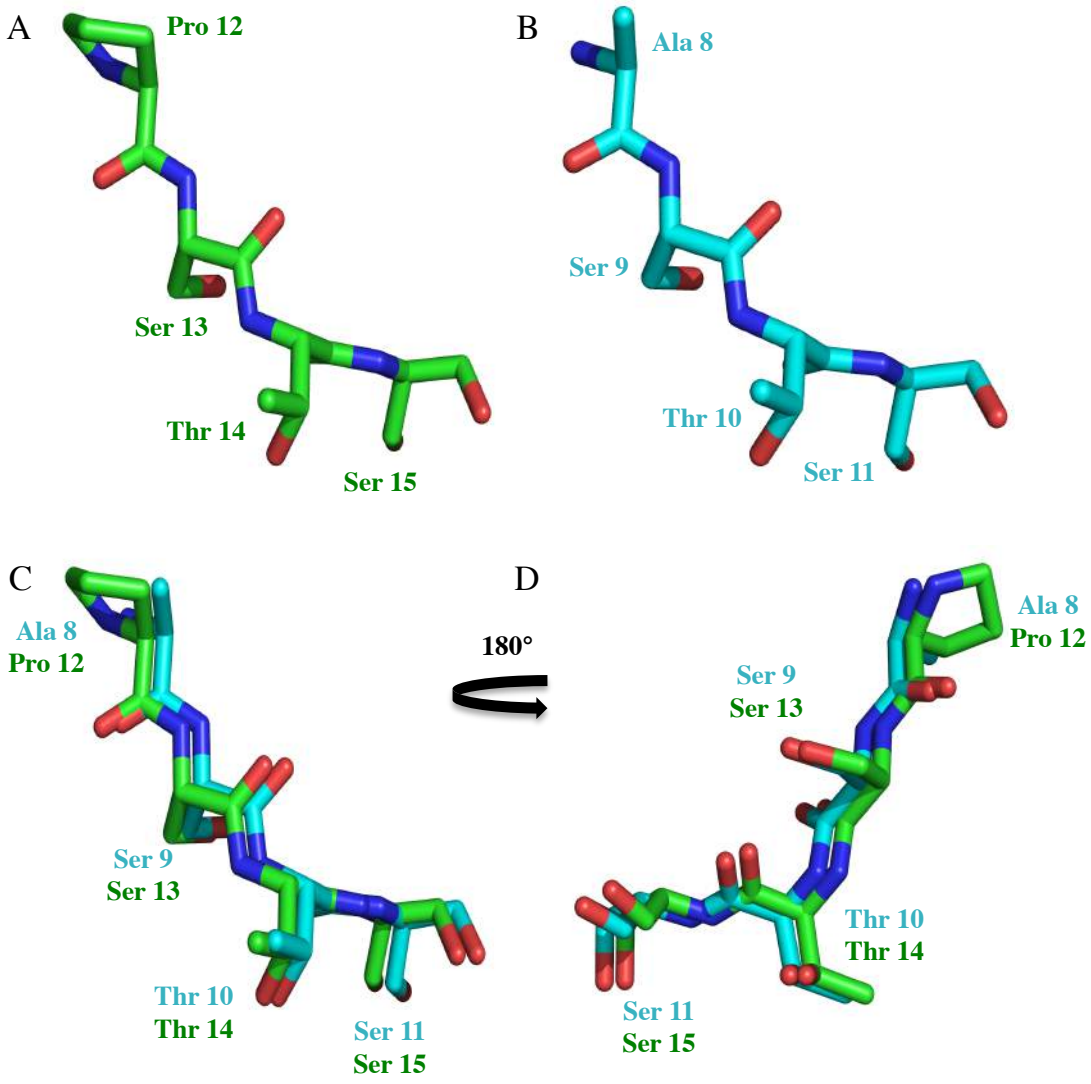

Figure 3.11: The USP7 binding motif of UbE2E2^{12}PSTS^{15} compared with that of UbE2E1^{8}ASTS^{11}. (A) Stick format of UbE2E2^{12}PSTS^{15} and (B) UbE2E1^{8}ASTS^{11} peptides showing all relevant residues. (C) Overlay of UbE2E2^{12}PSTS^{15} peptide (yellow) and UbE2E1^{8}ASTS^{11} peptide (cyan). All residues align perfectly, showing conserved interactions with USP7. (D) A rotated view of the overlay showing perfect alignment of the all residues. The difference of proline 12 in UbE2E2 (yellow) and alanine 8 in UbE2E1 (cyan) can be seen. Although the residues are different they completely align.

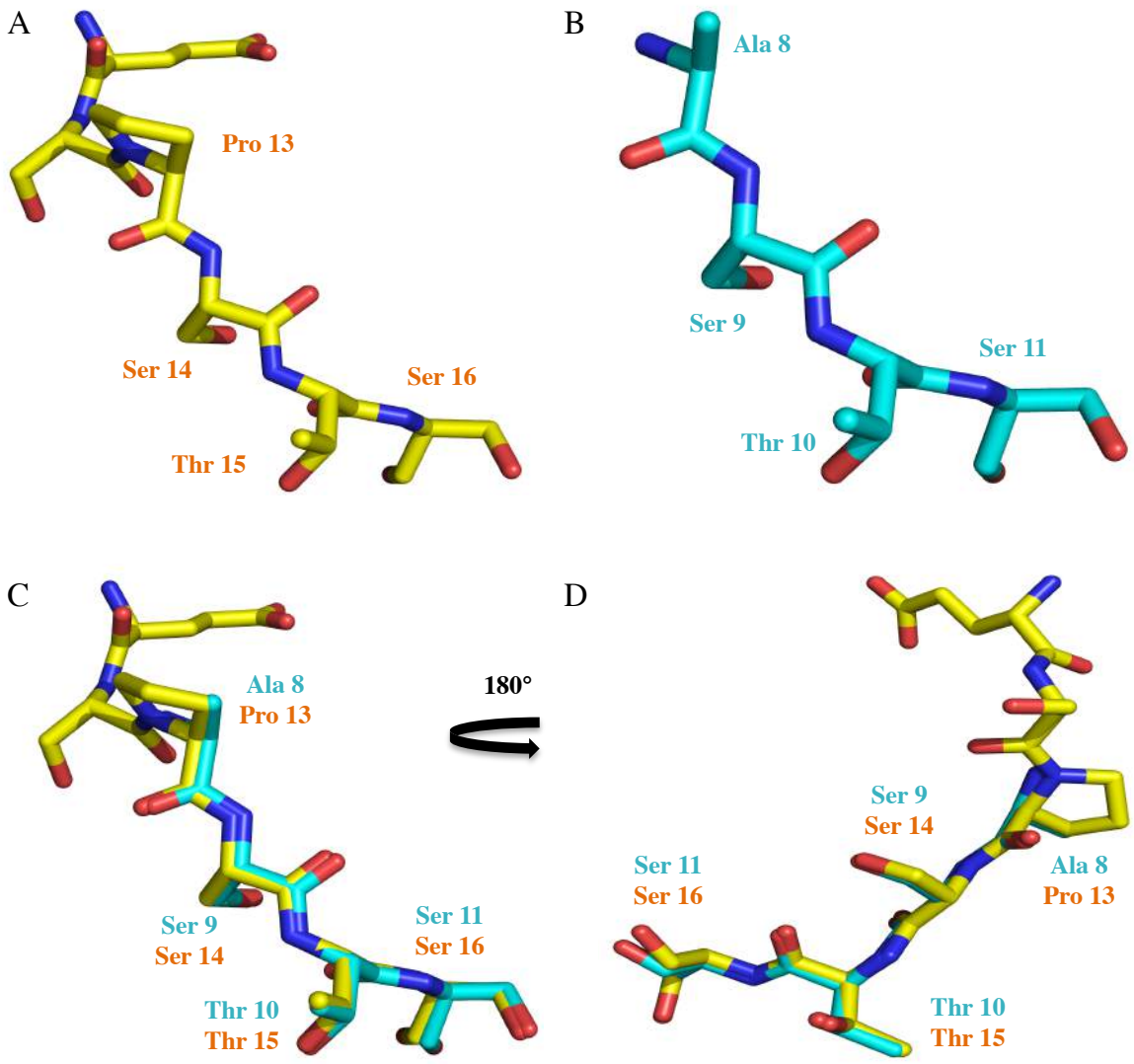

Figure 3.12: The USP7 binding motif of UbE2E3^{13}PSTS^{16} compared with that of UbE2E1^{8}ASTS^{11}. (A) Stick format of UbE2E3^{13}PSTS^{16} and (B) UbE2E1^{8}ASTS^{11} peptides showing all relevant residues. (C) Overlay of UbE2E3^{13}PSTS^{16} peptide (green) and UbE2E1^{8}ASTS^{11} peptide (cyan). All residues align completely, showing conserved interactions with USP7. (D) A rotated view of the overlay showing perfect alignment of the all residues. The difference of proline 13 in UbE2E3 (green) and alanine 8 in UbE2E1 (cyan) can be seen. Although the residues are different they completely align.

3.3 USP7 Regulates Cellular Levels of UbE2E2

USP7 is a de-ubiquitinating enzyme and can regulate cellular levels of its substrate by rescuing the substrate from ubiquitin-mediated degradation. Since UbE2E2 and UbE2E3 interact with USP7, we sought to investigate whether USP7 regulates their stability. Unfortunately, none of the antibodies tested were able to detect cellular levels of UbE2E3; therefore experiments were performed for UbE2E2 only. A protein turnover assay was performed using wild type human colon carcinoma (HCT116) cells and HCT116 USP7 -/-, in which the USP7 gene is deleted. The cells were incubated with 50μg/ml of cycloheximide for 2, 4, 8, 24 and 48 hours. Cells were harvested at each time interval to observe the levels of UbE2E2 using western blot analysis. Figure 3.13A shows that the cellular levels of UbE2E2, prior to cycloheximide treatment, are higher in wild-type HCT116 cells (lane 1) compared to USP7 -/- cells (lane 7). Following cycloheximide treatment, UbE2E2 levels steadily decrease throughout the 48-hour time interval but are not completely diminished after 48-hours in wild-type cells (Figure 3.13A). However, in USP7-/- cells, UbE2E2 levels remain constantly low after cycloheximide treatment and are diminished 48-hours post-treatment (Figure 3.13A). UbE2E2 levels post-CHX treatment were normalized against untreated cells (time point 0) and plotted on a line graph in Figure 3.13B. The slopes in Figure 3.13B indicate that the levels of UbE2E2 in HCT116 cells decrease more steadily after CHX treatment compared to HCT116 USP7 -/- cells.

In order to confirm that the reduced stability of UbE2E2 in HCT116 USP7-/- cells is due to the absence of USP7, we re- introduced USP7 into the HCT116 USP7-/- cells.

The transfection efficiency of the knockout cells is poor; therefore, we tested two transfection reagents to determine which would provide with a better transfection efficiency. Lipofectamine® 2000 Transfection Reagent provided for a better transfection efficiency (53%) than PolyJet™ *In Vitro* DNA Transfection Reagent (26%) (Figure 3.14). HCT116 USP7-/- cells were transfected with wild type USP7; a USP7 catalytic mutant in which the active site cysteine residue was mutated to a serine; and a USP7 binding mutant in which the residues ^{164}DW^{165} were mutated to alanine residues (Figure 3.15A, top panel). Compared to untransfected cells, cells transfected with wild type USP7 showed an increase in UbE2E2 levels (Figure 3.15 lane 1 and 2), suggesting that the absence of USP7 is responsible for the decreased stability of UbE2E2 in HCT116 USP7-/- cells. Furthermore, compared to untransfected cells, expression of USP7-CS led to a further decrease in UbE2E2 stability (Figure 3.15, lane 1 and 3). The results were similar for cells transfected with USP7-DW (Figure 3.15, lane 1 and 4). It should be noted that the transfection efficiency for HCT116 USP7 -/- cells was 53% (Figure 3.14). A higher transfection efficiency would have resulted in higher levels of UbE2E2 in the cell sample.

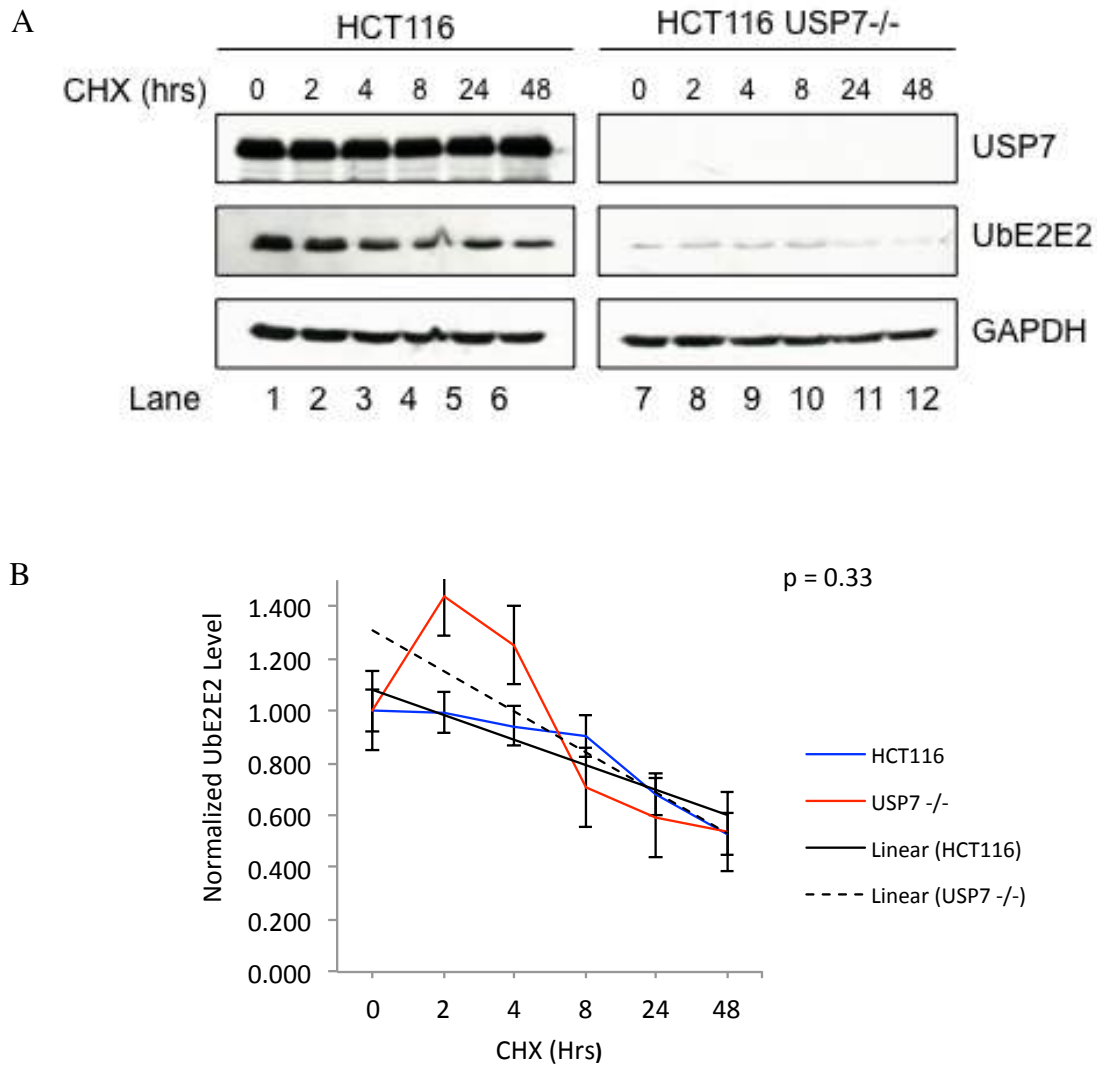

Figure 3.13: USP7 may regulate the cellular stability of UbE2E2. (A) HCT116 WT and HCT116 USP7 -/- cells were treated with 50ug/ml of cycloheximide. The cells were harvested 0, 2, 4, 8, 24 and 48 hours post-treatment and were analyzed by immunoblotting with antibodies against USP7, UbE2E2 and GAPDH. GAPDH was used as a loading control. (B) The levels of UbE2E2 in the experiment from (A) were normalized using UbE2E2 levels at time 0 as a loading control and presented using a line graph. The black line and the dashed line represent the line of best fit for HCT116 and USP7-/- cells, respectively. The error bars indicate standard error. The experiment was repeated twice (n = 2). A p-value of 0.33 was obtained. The error bars indicate standard error.

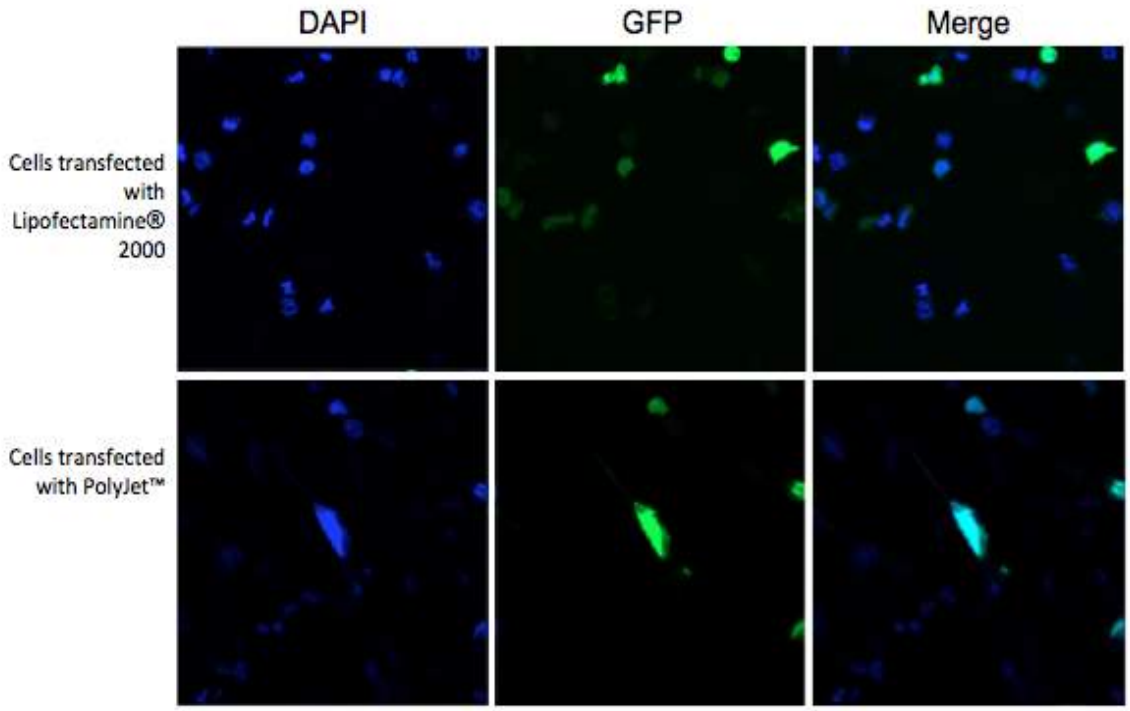

Figure 3.14: HCT116 USP7 -/- cells have low transfection efficiency. HCT116 USP7-/- cells were transfected with GFP using either Lipofectamine® 2000 Transfection Reagent or PolyJet™ *In Vitro* DNA Transfection Reagent. The cells were stained with DAPI reagent and observed under 40X objective using a Zeiss LSM 700 confocal microscope. Transfection efficiency was calculated by dividing the number of GFP-positive cells by the number of DAPI stained cells in the field of view.

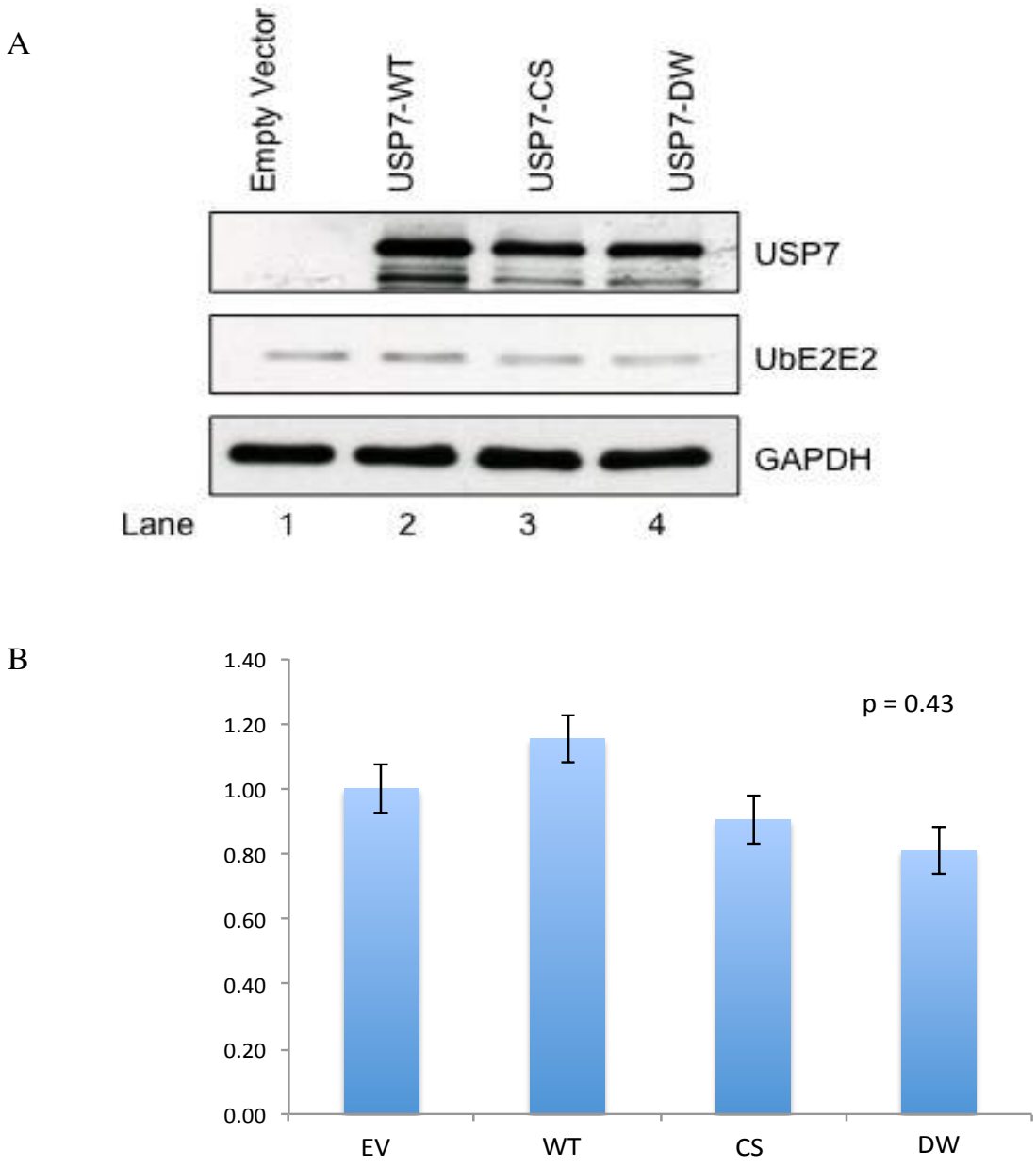

Figure 3.15: Analysis of cellular levels of UbE2E2 after reinstatement of USP7 into USP7-/- cells. (A) HCT116 USP7-/- cells were transfected using Lipofectamine® 2000 Transfection Reagent with either empty vector (EV), USP7-WT (WT), USP7-CS (CS) or USP7-DW (DW). The cells were lysed and blotted for UbE2E2 48 hours post-transfection. (B) The levels of UbE2E2 were normalized using empty vector levels of protein as a loading control. The experiment was repeated twice (n = 2). A p-value of 0.43 was obtained. The error bars indicate standard error.

CHAPTER 4: DISCUSSION

4.1 UbE2E2 and UbE2E3 Interact with USP7 *in vivo*

The class III ubiquitin-conjugating enzyme UbE2E1 shares a conserved UBC domain with UbE2E2 and UbE2E3. In addition, like UbE2E2 and UbE2E3, UbE2E1 harbors an N-terminal extension that contains a conserved P/AxxS motif. Sarkari et al. (2013) showed that USP7 was able to interact with UbE2E1 both *in vivo* and *in vitro*. Since UbE2E2 and UbE2E3 bear structural similarity to UbE2E1, we hypothesized that both proteins will interact with USP7. A preliminary study revealed that USP7 was able to interact with both UbE2E2 and UbE2E3 *in vitro*. Therefore, using a co-immunoprecipitation assay we sought to confirm these results *in vivo*. HEK293T cells were co-transfected with Flag-tagged UbE2E2 and Myc-tagged USP7. Our results show that Flag-UbE2E2 was detected in an immunoprecipitated complex with Myc-USP7 when cells were subjected to co-immunoprecipitation using either anti-Flag antibody or anti-Myc antibody (Figure 3.1), confirming that UbE2E2 interacts with USP7 *in vivo*.

A co-immunoprecipitation assay was repeated for cells co-transfected with Flag-UbE2E3 and Myc-USP7. Flag-UbE2E3 was detected in an immunoprecipitated complex with Myc-USP7 when cells were subjected to co-immunoprecipitation using either anti-Flag antibody or anti-Myc antibody (Figure 3.2), confirming that UbE2E3 also interacts with USP7 *in vivo*.

4.2 UbE2E2 and UbE2E3 bind the USP7-NTD at the shallow groove containing the β7-strand

In order to determine the mode of interaction between UbE2E2 and USP7 as well as UbE2E3 and USP7 we determined the tertiary structure of the peptide:protein complex using x-ray crystallography. The crystal structures of USP7:UbE2E2^{PSTS} and USP7:UbE2E3^{PSTS} were determined using molecular replacement to a resolution of 1.75Å and 2.00Å, respectively (Table 3.1). These high resolutions allowed us to model the hydrogen-bonding and surrounding water molecule networks along with the protein:peptide structure. The R_{work} and R_{free} values are 0.198 and 0.215 for UbE2E2 and 0.207 and 0.240 E2E3. They deviated by 2% for USP7:UbE2E2^{PSTS} and 4% for USP7:UbE2E3^{PSTS} indicating that the refined crystallographic structure is in agreement with the observed x-ray diffraction data. Furthermore, the Ramachandran Plot for both USP7:UbE2E2^{PSTS} and USP7:UbE2E3^{PSTS} indicates that 95.6% of the residues were in their most favored regions, further validating the accuracy of the determined crystal structures.

The crystal structure of USP7:UbE2E2^{PSTS} and USP7:UbE2E3^{PSTS} revealed that the UbE2E peptides bind to a shallow groove on the surface of the USP7-NTD containing the β7-strand (Figure 3.7 and Figure 3.8). The β7-strand of USP7 contains the binding motif ^{164}DWGF^{167}, which is essential for its interaction with substrate proteins containing the P/AxxS motif (Saridakis et al., 2005). Furthermore, preliminary studies revealed that a mutated USP7 in which Asp164 and Trp165 were changed to alanine residues failed to bind UbE2E2 and UbE2E3 in a GST-pull down (Mohamed et al., unpublished).

Together these results confirm that the interaction between UbE2E2 and USP7, as well as UbE2E3 and USP7, involves the ^{164}DWGF^{167} motif.

4.3 The PSTS motif in the N-terminal extension of UBE2E2 and UBE2E3 is involved the interaction with the USP7-NTD

The N-terminal extension of UbE2E2 and UbE2E3 contains a conserved PSTS motif. A preliminary study in our lab revealed that UbE2E2 and UbE2E3 proteins that lacked the N-terminal extension were unable to bind to USP7 in a GST pull down assay (Mohamed et al., unpublished). Using x-ray crystallography we were able to confirm that the interaction between UbE2E2:USP7, as well as UbE2E3:USP7 occurs between the PSTS motif in the N-terminal extensions of the UbE2Es and the ^{164}DWGF^{167} motif in the USP7-NTD β7-strand (Figure 3.9 and Figure 3.10). Specifically, Pro12 in UbE2E2 and Pro13 in UbE2E3 form Van der Waals interactions with USP7 Trp165 and Phe167 (Figure 3.9 and Figure 3.10). Ser13 in UbE2E2 and Ser13 in UbE2E3 make the most contacts with USP7. They form a water-mediated hydrogen bond with the main-chain amide of USP7 Ser168 and interact with the main-chain amide and carbonyl groups of USP7 Gly166 (Figure 3.9 and Figure 3.10). The serine residues at the fourth position in the P/AxxS motif, Ser15 in UbE2E2 and Ser16 in UbE2E3, form hydrogen bonds with the main chain and side chain of USP7 Asp164 (Figure 3.9 and Figure 3.10). This serine residue is most essential for binding to the USP7-NTD, as a mutation in this position in other USP7-NTD substrates such as UbE2E1 (Sarkari et al., 2013), p53 (Sheng et al., 2006) and EBNA1 (Saridakis et al., 2005) abolished the interaction.

The interaction between the UbE2Es and the USP7-NTD is identical to other USP7-NTD substrates that have been previously described, such as UbE2E1, p53 and Mdm2. An overlap of the UbE2E2 and UbE2E3 peptides with the UbE2E1 peptide is displayed in Figure 3.11 and Figure 3.12, respectively. Although the first proline in UbE2E2 and UbE2E3 is an alanine in UbE2E1, the peptides remain completely superposed, confirming that the interaction of these peptides with USP7 is conserved.

4.4 USP7 Regulates the Stability of UbE2E2

Sarkari et al. (2013) showed that USP7 was able to interact with and regulate the cellular levels of UbE2E1. Therefore, we hypothesized that because UbE2E2 and UbE2E3 bear structural resemblance to UbE2E1 and can interact with USP7, then USP7 should also be able to regulate the levels of UbE2E2 and UbE2E3. Figure 3.13A and B show that UbE2E2 levels are more stable in HCT116 wild type cells when compared to HCT116 USP7 -/- cells, suggesting that USP7 is required for the regulation and stability of the UbE2E2 protein. However, a p-value of 0.33 suggests that the results obtained are not significant. The high p-value obtained can be due to the small sample size used, as the experiment was only performed twice. If the experiment is repeated several times a lower p-value will be obtained.

Although our statistical analysis leads to the conclusion that USP7 is not regulating the stability of UbE2E2, we sought to determine how UbE2E2 levels would be affected if USP7 were reintroduced into the knockout cells using ectopic expression. When wild-type USP7 was reintroduced into knockout cells, UbE2E2 levels

were increased (Figure 3.15). The increase in UbE2E2 levels is dependent on the ability of USP7 to bind and deubiquitinate UbE2E2. This is consistent with the fact that ectopic expression of a USP7 catalytic mutant (USP7-CS) or USP7 binding mutant (USP7-DW) further reduced the levels of UbE2E2 in USP7 knockout cells (Figure 3.15). Moreover, it is important to note that knockout of USP7 does not completely abolish UbE2E2 levels, suggesting that there are other factors in the cell that may contribute to the regulation and stabilization of UbE2E2. The statistical analysis of this data set also suggests that the results are not statistically significant. This can also be attributed to the small sample size used, as the experiment was only performed twice.

4.5 Limitations of the research

Although we were able perform a protein turnover and rescue assay for UbE2E2, we were unable to do the same for UbE2E3. Our study was limited in this respect because none of the antibodies tested were able to detect endogenous levels of UbE2E3. We can overcome this limitation by developing an antibody against our protein of interest. Plafker *et al*. (2008) developed and purified a rabbit polyclonal antibody specific for the unique N-terminal extension of UbE2E3. Their self-developed antibody proved to be successful in detecting endogenous levels of UbE2E3 in various cell types including RPE cells and HeLa cells (Plafker *et al*., 2008; Mirza *et al*., 2010). We can continue with our studies for UbE2E3 once an antibody capable of detecting endogenous levels of UbE2E3 is developed.

Another limitation of our study was that our co-immunoprecipitations were

performed using two ectopically expressed proteins. Although the co-immunoprecipitations were successful in showing that UbE2E2 and UbE2E3 interact with USP7, our results would have been ideal if we have shown this interaction between the endogenous proteins. Unfortunately this could not be performed because we did not have an antibody to detect endogenous UbE2E3.

Finally, the transfection efficiency in our USP7 rescue assay was 53%. Therefore it is possible that the increase in UbE2E2 levels observed could have been greater if the transfection efficiency was higher. Sarkari et al. (2013) performed the same experiment to detect the levels of UbE2E1. Their transfection efficiency was also 50%, suggesting USP7 knockout cells may have poor transfection efficiency in general.

4.6 Significance of the research

DUBs have been shown to regulate the levels of E3 ligases. One example is USP7, which interacts with and stabilizes the E3 ligase Mdm2 (Li et al., 2004; Sheng et al., 2006). As well, the DUB USP8 interacts with and stabilizes the RING finger-containing E3 ligase Nrdp1 (Wu et al., 2004). However, there has not been much evidence of DUBs regulating other components of the ubiquitination cascade. A recent study by Sarkari et al. (2013) revealed that USP7 regulates the cellular levels of the E2 conjugating enzyme UbE2E1. The study by Sarkari et al. (2013) was the first to show that a DUB regulates an E2 conjugating enzyme.

In the current study we show that USP7 interacts with and may regulate another E2 conjugating enzyme, UbE2E2. We also show that USP7 interacts with the E2

conjugating enzyme UbE2E3 and that this interaction potentially leads to its stabilization in the cell. In order for ubiquitination machinery to work efficiently it must target substrates rather than target itself for degradation. Since USP7 was shown to regulate E2 conjugating enzymes, this study implicates USP7 as a guardian of the integrity of the ubiquitination machinery.

4.7 Future Directions

USP7 has been implicated in several cellular processes through its ability to interact with various substrates. For example, the interaction between USP7 and p53 has implicated USP7 in tumour suppression and the interaction between USP7 and EBNA1 has implicated USP7 in viral propagation. Here we show that USP7 interacts with two different E2 conjugating enzymes called UbE2E2 and UbE2E3. Aside from their role as ubiquitin conjugating enzymes not much has been discovered about the function of these two proteins. We can uncover the cellular function of UbE2E2 and UbE2E3 by identifying their substrates and interacting partners through use of mass spectroscopy. Once their cellular function is identified USP7 could be implicated in a greater amount of cellular functions, further justifying the importance and multi-functional character of this protein.

CHAPTER 5: CONCLUSION

The objective of this project was threefold; first we wanted to determine whether UbE2E2 and UbE2E3 are able to interact with USP7 *in vivo*. Second, we wanted to determine the molecular details of interaction between USP7 and UbE2E2, as well as USP7 and UbE2E3. Finally, we wanted to study the effect of the interaction between USP7 and the UbE2E proteins. Using a co-immunoprecipitation assay it was established that USP7 interacts with both UbE2E2 and UbE2E3 *in vivo*. These results further validate the *in vitro* interaction observed between USP7 and UbE2E2, as well as USP7 and UbE2E3 in a preliminary study. Furthermore, the crystal structure of USP7:UbE2E2, as well as USP7:UbE2E3, demonstrated that the PSTS motif in both UbE2E2 and UbE2E3 binds to a shallow groove on the surface of the USP7-NTD, which contains the β-strand residues ^{164}DWGF^{167}. A major contact was established between Ser15 in UbE2E2 and Asp164 in USP7, as well as Ser16 in UbE2E3 and Asp164 in USP7. The effect of the interaction between USP7 and UbE2E2 was studied using a protein turnover assay, which indicated that USP7 may regulate the cellular levels of UbE2E2. This study identifies an additional E2 conjugating enzyme that is regulated by the DUB USP7.

REFERENCES

Burroughs AM, Jaffee M, Iyer LM and Aravind L. 2008. Anatomy of the E2 ligase fold: implication for enzymology and evolution of ubiquitin/Ub-like protein conjugation. *J Struct Biol* 162(2): 205-218.

David Y, Ziv T, Admon A and Navon A. 2010. The E2 ubiquitin-conjugating enzymes direct polyubiquitination to preferred lysines. *J Biol Chem* 285: 8595-8604.

David Y, Ternette N, Edelmann MJ, Ziv T, Gayer B, Sertchook R, Dadon Y, Kessler BM and Navon A. 2011. E3 ligases determine ubiquitination site and conjugate type by enforcing specificity on E2 enzymes. *J Biol Chem* 286: 44104-44115.

Daubeuf S., Singh D., Tan Y., Liu H., Federoff HJ., Bowers WJ. and Tolba K. 2009. HSV ICP0 recruits USP7 to modulate TLR-mediated innate response. *Blood* 113(14): 3264-3275.

Everett RD., Meredith M., Orr A., Cross A., Kathoria M. and Parkinson J. 1997. A novel ubiquitin-specific protease is dynamically associated with the PML nuclear domain and binds to herpesvirus regulatory protein. *EMBO J* 16(7): 1519-1530.

Faesen AC., Dirac AM., Shanmugham A., Ovaa H., Perrakis A., and Sixma TK. 2011. Mechanism of USP7/HAUSP activation by its C-terminal ubiquitin-like domain and allosteric regulation by GMP-synthetase. *Mol Cell* 44(1): 147-259.

Faesen AC., Luna-Vargas MPA. and Sixma TK. 2012. The role of UBL domains in ubiquitin-specific proteases. *Biochem Soc Trans* 40: 539-545.

Goldstein G, Scheid M, Hammerling U, Boyse EA, Schlesinger DH and Naill HD. 1975. Isolation of a polypeptide that has lymphocyte-differentiating properties and is probably represented universally in living cells. *Proc Nat Acad Sci USA* 72(1): 11-15.

Hu M., Li P., Li M., Li W., Yao T., Wu J., Gu W., Cohen RE., and Shi Y. 2002. Crystal structure of a UBP-Family deubiquitinating enzyme in isolation and in complex with ubiquitin aldehyde. *Cell* 111: 1041-1054.

Ito K, Adachi S, Iwakami R, Yasuda H, Muto Y, Seki N and Okano Y. 2001. N-terminally extended human ubiquitin-conjugating enzymes (E2s) mediate the ubiquitination of RING-finger proteins ARA54 and Rnf8. *Eur J Biochem* 268: 2725-2732.

Jagannathan M., Nguyen T., Gallo D., Luthra N., Brown GW., Saridakis V. and Frappier L. 2014. A role for USP7 in DNA replication. *Mol Cell Biol* 34(1): 132-145.

Komander D. 2009. The emerging complexity of protein ubiquitination. *Biochem Soc T* 37: 937-953.

Kim JH., Park KC., Chung SS., Bang O., and Chung CH. 2003. Deubiquitinating Enzymes as Cellular Regulators. *J Biochem* 134:9-18.

Kim JY., Cheong HS., Park Bl., Baik SH., Park S., Shin HD., and Kim SH. 2013. Putative association between UBE2E2 polymorphisms and the risk of gestational diabetes mellitus. *Gynecol Endocrinol* 29 (10): 904-908.

Kimura Y and Tanaka K. 2010. Regulatory mechanisms involved in the control of ubiquitin homeostasis. *J Biochem* 147 (6): 793-798.

Li M., Chen D., Shiloh A., Luo J., Nokolaev AY., Qin J and Gu Wei. 2002. Deubiquitination of p53 by HAUSP is an important pathway for p53 stabilization. *Nature* 416: 648-653.

Li M., Brook CL., Kon N. and Gu W. 2004. A dynamic role of HAUSP in the p53-Mdm2 pathway. *Mol Cell* 13: 879-886.

Li W, Tu D, Brunger AT and Ye Y. 2007. A ubiquitin ligase transfers preformed polyubiquitin chains from a conjugating enzyme to a substrate. *Nature* 446: 333-337.

Matuschewski K, Hauser HP, Treier M and Jentsch S. 1996. Identification of a novel family of ubiquitin-conjugating enzymes with distinct amino-terminal extensions. *J Biol Chem* 271(5): 2789-2794.

Meredith, MR., Orr A. and Everett RD. 1994. Herpes Simplex Virus Type 1 immediate-early protein Vmv110 binds strongly and specifically to a 135kD cellular protein. *Virology* 200: 457-469.

Mirza S., Plafker KS., Aston C. and Plafker SM. 2010. Expression and distribution of the class III ubiquitin-conjugating enzymes in the retina. *Mol Vis* 16: 2425-2437.

Moll UM and Petrenko O. 2003. The Mdm2-p53 interaction. *Mol Cancer Res* 1: 1001-1008.

Passmore JA and Barford D. 2004. Getting into position: the catalytic mechanisms of protein ubiquitylation. *Biochem J* 379: 513-525.

Peng J, Schwartz D, Elias JE, Thoreen CC, Cheng D, Marsischky G, Roelofs J, Finley D and Gygi SP. 2003. A proteomics approach to understanding protein ubiquitination. *Nat Biotechnol* 21(8); 921-926.

Pickart CM. (2001). Mechanisms underlying ubiquitination. *Annu Rev Biochem* 70: 503-533.

Plafker KS., Farjo KM., Wiechmann AF. and Plafker SM. 2008. The human ubiquitin conjugating enzyme UBE2E3 is required for proliferation of retinal pigment epithelial cells. *Invest Ophth Vis Sci* 49(12): 5611-5618.

Plafker KS., Nguyen L., Barneche M., Mirza S., Crawford D., and Plafker SM. 2010. The ubiquitin-conjugating enzyme UbcM2 can regulate the stability and activity of the antioxidant transcription factor Nrf2. *J Biol Chem* 285(30): 23064-23074.

Plafker KS., Singer JD. and Plafker SM. 2009. The ubiquitin-conjugating enzyme, UbcM2, engages in novel interactions with components of cullin-3 based E3 ligases. *Biochem* 48: 3527-3537.

Plafker SM, Plafker KS, Weissman AM and Macara IG. 2004. Ubiqiuitin charging of huan class III ubiquitin-conjugating enzymes triggers their nuclear import. *J Cell Biol* 167(4): 649-659.

Reyes-Turcu FE., Ventii KH. and Wilkinson KD. 2009. Regulation and cellular roles of ubiquitin-specific deubiquitinating enzymes. *Annu Rev Biochem* 78: 363-397.

Sarkari F., La Delfa A., Arrowsmith CH., Frappier L., Sheng Y., and Saridakis V. 2010. Further insight into substrate recognition by USP7: structural and biochemical analysis of the HdmX and Hdm2 interactions with USP7. *J Mol Biol* 402: 825– 837.

Sarkari F., Wheaton K., La Delfa A., Mohamed M., Shaikh F., Khatun R., Arrowsmith CH., Frappier L., Saridakis S. and Sheng Y. 2013. Ubiquitin-specific protease 7 is a regulator of ubiquitin-conjugating enzyme UbE2E1. *J Biol Chem* 288(33): 16975-16985.

Saridakis V., Sheng Y., Sarkari F., Holowaty MN., Shire K., Nguyen T., Zhang RG., Liao J., Lee W., Edwards AM., Arrowsmith CH and Frappier L. 2005. Structure of the p53 binding domain of HAUSP/USP7 bound to Epstein-Barr Nucleat Antigen 1: implication for EBV-mediated immortalization. *Mol Cell* 18: 25-36.

Sheng Y., Saridakis V., Sarkari F., Duan S., Wu T., Arrowsmith CH., and Frappier L. 2006. Molecular recognition of p53 and MDM2 by USP7/HAUSP. *Nat Struct Mol Biol* 13(3): 285-291.

van der Knaap JA., Kumar BRP., Moshkin YM., Langenberg K., Krijgsveld J., Heck AJR., Karch F. and Verrijzer CP. 2005. GMP synthetase stimulates histone H2B deubiquitylation by the epigenetic silencer USP7. *Mol Cell* 17(5): 695-707.

van Wiljk SJ. and Timmers HT. 2010. The family of ubiquitin-conjugating enzymes (E2s): deciding between life and death of proteins. *FASEB J* **24** (4): 981–93.

Wenzel DM., Stroll KE. and Klevit RE. 2011. E2s: structurally economical and functionally replicate. *J Biochem* 433: 31-42.
Wu X., Yen L., Irwin L, Sweeney C., and Carraway KL. 2004. Stabilization of the E3 ubiquitin ligase Nrdp1 by the deubiquitinating enzyme USP8. *J Mol Cell Biol* 24(17): 7748-7757.

Zhu B., Zheng Y., Pham AD., Mandal SS., Erdjument-Bromage H., Tempst P., Reinberg D. 2005. Monoubiquitination of human histone H2B: the factors involved and their roles in HOX gene regulation. *Mol Cell* 20: 601-611.